FINNISH METEOROLOGICAL INSTITUTE
CONTRIBUTIONS
No. 191

Insights into the above- and belowground CO_2 fluxes on pristine and managed peatlands: tools for examining ecosystem carbon cycle

Maiju Linkosalmi

Doctoral Programme in Sustainable Use of Renewable Natural Resources
Department of Forest Sciences
Faculty of Agriculture and Forestry
University of Helsinki

Academic dissertation presented for the degree of
Doctor of Science in Agriculture and Forestry

To be presented for public examination with the permission of
the Faculty of Agriculture and Forestry of the University of Helsinki
in the Auditorium B123, Pietari Kalmin katu 5, Helsinki,
on 1st of December 2023 at 12 o'clock

Finnish Meteorological Institute
Helsinki 2023

Author's contact: Climate System Research, Finnish Meteorological Institute,
PL 503, FI-00101 Helsinki, Finland
maiju.linkosalmi@fmi.fi
https://orcid.org/0000-0002-5712-6769

Supervisors: Professor Annalea Lohila, Ph.D.
Climate System Research, Finnish Meteorological Institute
Institute for Atmospheric and Earth System Research (INAR),
University of Helsinki

Mika Aurela, Ph.D.
Climate System Research, Finnish Meteorological Institute

Assistant Professor Christina Biasi, Ph.D.
Department of Environmental and Biological Sciences, University of Eastern Finland
Department of Ecology, University of Innsbruck

Reviewers: Christopher Poeplau, PD Dr. rer. nat.
Thünen Institute of Climate-Smart Agriculture

Docent Teemu Tahvanainen, Ph.D.
Department of Environmental and Biological Sciences, Faculty of Science, Forestry and Technology, University of Eastern Finland

Opponent: Professor of Biogeochemistry Lisa Belyea, Ph.D.
School of Geography, Queen Mary University of London

Custos: Professor Annamari Laurén, Ph.D.
Department of Forest Sciences, Faculty of Agriculture and Forestry,
University of Helsinki

ILMATIETEEN LAITOS
METEOROLOGISKA INSTITUTET
FINNISH METEOROLOGICAL INSTITUTE

Published by **Finnish Meteorological Institute**
(Erik Palménin aukio 1)
P.O. Box 503
FIN-00101 Helsinki, Finland

Series title, number and report code of publication
FMI Contributions, 191, FMI-CONT-191

December 2023

Author

Maiju Linkosalmi

ORCID iD

https://orcid.org/0000-0002-5712-6769

Title

Insights into the above- and belowground CO_2 fluxes on pristine and managed peatlands: tools for examining ecosystem carbon cycle

Abstract

Climate change and land-use changes modify the conditions and characteristics of northern peatlands and thus affect their carbon (C) balance. In this thesis the above- and belowground carbon dioxide (CO_2) fluxes of peatland ecosystems were examined with process-specific methods. These methods provide additional information and support the standardized measurements. Phenology cameras were used for observing the seasonal development and greenness of vegetation at different ecosystems (pristine peatlands and a forest site). This vegetation phenology data was combined with CO_2 flux measurements, meteorological data and satellite-derived data. Also, the soil CO_2 fluxes and priming effect (PE), i.e., the change in decomposition of soil after addition of fresh C, were studied in laboratory experiments with isotope techniques. The peat for these experiments was collected from two forestry-drained peatlands with different nutrient status.

The phenology cameras were found to be a solid method for tracking changes in ecosystem greenness. Variations in vegetation dynamics were observed between different study years as well as between different ecosystems and plant communities within a peatland. These differences in vegetation greenness were linked to nutrient availability and vegetation composition of the site or the region of interest. The peatland vegetation also compensated for the late growing season start: during a summer with the latest growing season start the vegetation was capable to reach the maximum GCC and maximal photosynthetic activity over the measurement years. The effect of drought on greenness and maximal photosynthetic activity was found to depend on the hydrological features of the site. The camera- and satellite-derived greenness index showed similar seasonal cycle, but the poorer temporal resolution of the satellite data affected the reliable determination of the timing of different phenological phases.

The results of the laboratory studies indicated that the nutrient-rich peat had higher basal peat respiration rate and also higher peat respiration in the presence of plants. The results are in accordance with the observed differences in the CO_2 balances at the sites from which the peat samples were collected: the nutrient-rich peat soil has been observed to lose C and the nutrient-poor peat accumulate C. No priming or negative priming was found in these studies. Thus, it can be concluded that the addition of fresh C (in the form of seedling roots or glucose) did not increase, or it even decreased, the old peat decomposition in these peat soils. The negative priming was stronger in the peat soil with less nutrients available.

Publishing unit

Climate System Research

Classification (UDC)

504.7, 581.5, 631.42

Keywords

Carbon dioxide, vegetation greenness, phenology, phenology camera, satellite, peatland, forestry-drained peatland, peat decomposition, priming effect

ISSN and series title

0782-6117 (print)
2814-5658 (online)
Finnish Meteorological Institute Contributions

ISBN

978-952-336-184-3 (print)
978-952-336-185-0 (online)

DOI

https://doi.org/10.35614/isbn.9789523361850

Language

English

Pages

60

ILMATIETEEN LAITOS
METEOROLOGISKA INSTITUTET
FINNISH METEOROLOGICAL INSTITUTE

Julkaisija **Ilmatieteen laitos**
(Erik Palménin aukio 1)
PL 503
00101 Helsinki

Julkaisun sarja, numero ja raporttikoodi
FMI Contributions, 191, FMI-CONT-191

Joulukuu 2023

Tekijä

Maiju Linkosalmi

ORCID iD

https://orcid.org/0000-0002-5712-6769

Nimeke

Näkemyksiä luonnontilaisten ja käsiteltyjen turvemaiden maanpäällisistä ja maanalaisista hiilidioksidivirroista: työkaluja ekosysteemin hiilenkierron tarkasteluun

Tiivistelmä

Muuttuva ilmasto ja maankäytön muutokset muokkaavat pohjoisten turvemaiden olosuhteita ja ominaispiirteitä, ja siten vaikuttavat niiden hiilitaseeseen. Tässä väitöskirjassa tutkittiin maanpäällisiä ja maanalaisia hiilidioksidivirtoja prosessikohtaisilla menetelmillä. Näillä menetelmillä tutkituista prosesseista voidaan tuottaa lisätietoa, jota voidaan käyttää standardoitujen mittauksien tukena. Erilaisten ekosysteemien kasvillisuuden kehitystä ja vihreyttä havainnoitiin fenologiakameroiden avulla. Tätä aineistoa yhdistettiin hiilidioksidimittausten, meteorologisten mittausten ja satelliittiaineistojen kanssa. Lisäksi turpeen hiilidioksidivuota ja priming effectiä tarkasteltiin laboratoriokokeissa isotooppimenetelmien avulla. Priming effectillä tarkoitetaan maaperän vanhan orgaanisen aineen hajotuksessa tapahtuvaa muutosta, kun maahan lisätään helposti hajotettavaa tuoretta orgaanista ainesta. Turve näitä laboratoriokokeita varten kerättiin kahdelta metsäojitetulta suolta.

Fenologiakamerat osoittautuivat luotettavaksi menetelmäksi ekosysteemin vihreyden ja sen kehityksen havainnointiin. Sekä erilaisten ekosysteemien, kasvillisuusryhmien, että vuosien välillä havaittiin eroavaisuuksia. Näiden eroavaisuuksien todettiin liittyvän tutkittavien kohteiden ravinteiden saatavuuteen ja kasvillisuuden ominaisuuksiin. Suokasvillisuus oli myös kykenevä kompensoimaan kasvuaan myöhemmin kesän aikana huolimatta kasvukauden alun viivästymisestä. Kuivuuden vaikutus kasvillisuuden vihreyteen ja fotosynteettiseen aktiivisuuteen riippui suon hydrologisista ominaispiirteistä. Kameroista ja satelliitista johdetuilla vihreysindekseillä oli samanlainen kausittainen vaihtelu, mutta huonomman ajallisen resoluution vuoksi erilaisten fenologisten vaiheiden määrittäminen satelliittidatasta oli epäluotettavampaa.

Laboratoriokokeiden tulokset osoittivat, että hajotus oli suurempaa ravinteikkaammassa turpeessa. Nämä tulokset ovat yhdenmukaisia aiempien havaintojen kanssa, joiden mukaan ravinteikkaamman metsäojitetun suon maaperä on hiilen lähde ja vähäravinteisen metsäojitetun suon maaperä hiilen nielu. Näissä tutkimuksissa ei havaittu priming effectiä tai se oli negatiivista. Siten voidaan päätellä, että tuoreen hiilen lisäys ei lisännyt, vaan jopa vähensi, vanhan hiilen hajotusta näillä turvemailla. Negatiivinen priming effect oli lisäksi voimakkaampaa vähäravinteisessa turpeessa.

Julkaisijayksikkö

Ilmastojärjestelmätutkimus

Luokitus (UDK)

504.7, 581.5, 631.42

Asiasanat

Hiilidioksidi, kasvillisuuden vihreys, fenologia, fenologiakamera, satelliitti, suo, metsäojitettu suo, turpeen hajotus, priming effect

ISSN ja avainnimeke

0782-6117 (painettu)
2814-5658 (verkkojulkaisu)
Finnish Meteorological Institute Contributions

ISBN

978-952-336-184-3 (painettu)
978-952-336-185-0 (verkkojulkaisu)

DOI

https://doi.org/10.35614/isbn.9789523361850

Kieli

englanti

Sivumäärä

60

Acknowledgements

Building this thesis has been a long and eventful process, but here it finally is! I would like to express my gratitude to everyone who has contributed to this journey. This thesis represents not only my efforts, but also the work and support of many people and institutions.

First and foremost, I want to thank my supervisors Annalea Lohila, Mika Aurela and Christina Biasi, whose expertise and resourcefulness have made this thesis possible. Thanks for your patience and support through many twists and turns.

I would like to acknowledge all my co-authors: Juha-Pekka Tuovinen, Mikko Peltoniemi, Cemal M. Taniş, Ali N. Arslan, Pasi Kolari, Kristin Böttcher, Tuula Aalto, Juuso Rainne, Juha Hatakka, Olli Nevalainen, Tuomas Laurila, Jukka Pumpanen, Jussi Heinonsalo, Raija Laiho, Aki Lindén and Vesa Palonen. Special thanks to J-P for helping with scientific and grammar related problems, your input greatly improved this thesis.

I am also grateful to Maj and Tor Nessling foundation and Monimet EU Life+ project for financial support.

I wish to thank the pre-examiners Teemu Tahvanainen and Christopher Poeplau for reviewing this thesis and for valuable comments and suggestions. I am grateful to Professor Lisa Belyea for accepting to act as the opponent and professor Annamari Laurén for acting as the Custos.

I wish to express my appreciation to our former and current group leaders Tuomas and Hermanni for all your support and trust. My gratitude also goes to all my colleagues in the greenhouse gases and carbon cycle groups for all the work related and free time activities. Thank you especially Aki, Tiina, Sari, Tuula and Mika K. for mentoring along the way.

I also want to thank my friends for all the good times, from childhood suburban forests to bigger adventures. I am very grateful to my dearest family members for their support: mum, dad, Anni and Lauri and their families. And lastly, thank you Tommi, Ilja and Siiri for putting things into perspective and bringing so much joy.

TABLE OF CONTENTS

List of publications

This thesis consists of an introductory review followed by four research articles. **Papers I**, **II** and **IV** are printed under the Creative Commons Attribution license (3.0 or 4.0) and **Paper III** is reprinted with the kind permission of the publisher.

I **Linkosalmi, M.**, Aurela, M., Tuovinen, J.-P., Peltoniemi, M., Taniş, C. M., Arslan, A. N., Kolari, P., Böttcher, K., Aalto, T., Rainne, J., Hatakka, J., Laurila, T.: Digital photography for assessing the link between vegetation phenology and CO_2 exchange in two contrasting northern ecosystems. *Geoscientific Instrumentation, Methods and Data Systems.*, 5:417–426, 2016. https://doi.org/10.5194/gi-5-417-2016

II **Linkosalmi, M.**, Tuovinen, J.-P., Nevalainen, O., Peltoniemi, M., Taniş, C. M., Arslan, A. N., Rainne, J., Lohila, A., Laurila, T., Aurela, M.: Tracking vegetation phenology of pristine northern boreal peatlands by combining digital photography with CO_2 flux and remote sensing data. *Biogeosciences,* 19: 4747–4765, 2022. https://doi.org/10.5194/bg-19-4747-2022

III **Linkosalmi, M.**, Pumpanen, J., Biasi, C., Heinonsalo, J., Laiho, R., Lindén, A., Palonen, V., Laurila, T., Lohila, A.: Studying the impact of living roots on the decomposition of soil organic matter in two different forestry-drained peatlands. *Plant Soil*, 396: 59–72, 2015. https://doi.org/10.1007/s11104-015-2584-4

IV **Linkosalmi, M.**, Lohila, A., Biasi, C.: Stronger negative priming effect and lower basal respiration rates in nutrient-poor as compared to nutrient-rich forestry-drained peatland. *Rapid Communications in Mass Spectrometry*, 37: e9540, 2023. https://doi.org/10.1002/rcm.9540

Author's contribution

I In this article, the author participated in setting up of the digital cameras and performed the image data analysis. The author was the principal author and wrote the paper with contributions from all co-authors. This paper has not been or will not be used in any other PhD thesis.

II In this article, the author was responsible for image data analysis and combining this data with other data sets. The author acted as the principal author and wrote the paper with contributions from all co-authors. This paper has not been or will not be used in any other PhD thesis.

III In this article, the author carried out the laboratory measurements and data analysis. The author acted as the principal author and wrote the paper with contributions from all co-authors. This paper has not been or will not be used in any other PhD thesis.

IV In this article, the author carried out the laboratory measurements and data analysis. The author acted as the principal author and wrote the paper with contributions from all co-authors. This paper has not been or will not be used in any other PhD thesis.

1. Introduction

1.1. Background

Compared to other ecosystems, peatlands are characterized by a high water table (e.g., Rydin and Jeglum 2013), which often is a result of poor soil surface transmissivity and flat topography (Gorham 1991). This leads to specific peatland vegetation, anoxic soil conditions, low primary production and limited decomposition (Frolking et al. 1998, Bubier et al. 1999, Moore and Basiliko 2006). In peatlands, biomass production exceeds soil decomposition and thus leads to the accumulation of organic matter, referred to as peat (e.g., Kuhry and Turunen 2006). As organic matter, peat consists mostly of carbon (C).

The majority of the present-day peatland ecosystems are located in the northern hemisphere, mostly in boreal and subarctic regions, and have been formed during the last 11,000 years, after the last glacial period (Gajewski et al. 2001). The high-latitude climate zones have a humid climate, where precipitation exceeds transpiration, and thus the conditions are favourable for peatland formation. Peatland formation is still an ongoing, self-enhancing geological process (Vitt and Wieder 2006).

Globally, peatlands cover about 3% (4×10^6 km^2) of the land area (Xu et al. 2018) and the proportion of boreal and subarctic peat soils within this area has been estimated to be almost 90% (3.46×10^6 km^2, Gorham 1991). Especially northern peatlands constitute a large C storage, estimated to contain up to a third of the global soil C (Gorham 1991). In Finland, peat soils contribute about 30% (~96,000 km^2) of the total land area (Turunen et al. 2002, Turunen 2008). Two-thirds of the natural state peatlands in Finland have been drained, mainly for forestry (Päivänen and Hånell 2012).

The nutrient status of peatlands usually depends on the hydrological features of the peatland ecosystem. Generally, boreal and subarctic pristine peatlands can be classified by their nutrient status. Fens are in direct contact with groundwater and thus they gain nutrients from surrounding mineral soils as well as from rainwater. By contrast, precipitation is the only source of nutrients for the bog vegetation, and therefore the nutrient availability is lower in bogs than in fens (Rydin and Jeglum 2013). Bogs are typically dominated by *Sphagnum* moss, shrubs and sedges, while fens are dominated by sedges and grasses (e.g., Harenda et al. 2018). The nutrient availability affects ecosystem processes by dictating the vegetation composition of the peatland and thus also has an effect on primary production. Furthermore, the nutrient status has an impact on the physical and chemical peat characteristics, which affect the microbial communities and decomposition processes (Moore 2002). A more recalcitrant, e.g., *Sphagnum*-dominated, vegetation results in more acidic peat, lower nutrient concentration and higher carbon-to-nitrogen (C/N) ratio, which makes the peat more resistant to decomposition (Scheffer and Aerts 2000, Moore 2002).

Northern pristine peatlands sequester atmospheric carbon dioxide (CO_2) and emit methane (CH_4), which are the key greenhouse gases, and are typically net sinks of C (Gorham 1991, Clymo et al. 1998, Turunen et al. 2002, Limpens et al. 2008). Climate change and related land-use changes have an effect on the C balance of northern peatlands, especially within the permafrost region. Even though atmospheric warming may degrade permafrost and induce droughts decreasing the C sink of peatlands (Crowther et al. 2016, Harenda et al. 2018), the high-latitude peatlands have also been suggested to accumulate more peat in warmer conditions and thus increase the C storage due to greater plant growth (Jones et al. 2017, Gallego-Sala et al. 2018, Loisel et al. 2021). Improved understanding of the interactions between hydrology, surface structure and peat formation is needed to predict climate-change-driven feedbacks that the peatlands may have on the global C cycle (Turetsky et al. 2002, Belyea and Malmer 2004).

Human-induced land-use changes also modify conditions and characteristics of northern peatlands, which in turn affect the C balance. For example, when the water table drops due to forestry drainage, the soil decomposition, tree photosynthesis and litter production increase, and in addition vegetation and the quality of litter change (Laiho et al. 2003, Laiho 2006, Minkkinen et al. 1999, Strakova et al. 2010). The effect of drainage on the C balance depends on the original peatland type and the properties of the soil (Minkkinen et al. 1999, Jaatinen et al. 2007, Peltoniemi et al. 2009, 2012). The drained fens with higher decomposition rates have been reported to act as sources of C to the atmosphere (e.g., Ojanen et al. 2013, 2014, Krüger at al. 2016), while there is evidence that drained bogs can remain as C sinks or have a close-to-neutral C balance (Lohila et al. 2011, Ojanen et al. 2013, 2014, Krüger at al. 2016). From a productivity point of view, the more nutrient-rich sites are better environments for vegetation growth, and thus they are used more commonly for drainage for forestry and agriculture. Pristine northern peatlands are CO_2 sinks, while drained peatlands can further act as a sink or turn into a source of CO_2 (Minkkinen and Laine 1998, Maljanen et al. 2010, Lohila et al. 2011, Simola et al. 2012, Ojanen et al. 2013). Besides the CO_2 emissions, C losses from peat soil occur mainly by CH_4 release and dissolved organic carbon (DOC) leaching (Moore et al. 1998, Aitkenhead and McDowell 2000). CH_4 is formed in anoxic conditions (Rydin and Jeglum 2013) and thus CH_4 emissions are reduced if the peatland is drained (Martikainen et al. 1995). In this thesis, the focus is on the ecosystem CO_2 fluxes.

1.2. Definition of the ecosystem CO_2 balance

1.2.1. Components of the CO_2 balance

The CO_2 balance of an ecosystem is defined as the difference between the flux components produced by plant photosynthesis and ecosystem respiration. To determine and understand this balance and its total effect on atmospheric interactions, processes occurring both aboveground and belowground must be examined. Like other ecosystems, peatlands fix CO_2 in the photosynthesis by plants and release it

by respiration processes; as a result, C is stored in the vegetation and peat soil as organic matter (e.g., Rydin and Jeglum 2013). The rate of photosynthesis is controlled by many environmental factors, such as solar radiation, air temperature and the availability of water and nutrients (e.g., Keys et al. 1994, Fatichi et al. 2014). Vegetation releases CO_2 through respiration processes involved in the growth and maintenance of aboveground and belowground plant parts. In addition, CO_2 is released from peat soil through the respiration of decomposers, such as soil animals and microbial communities (e.g., Vasander and Kettunen 2006).

The exchange of CO_2 between an ecosystem and the atmosphere can be determined in different ways. A widely used technique for directly measuring the net ecosystem CO_2 exchange (NEE) is the micrometeorological eddy covariance (EC) method. The EC method produces continuous CO_2 flux data that is spatially averaged on the ecosystem scale. To better understand the controls of the total CO_2 balance, it is important to partition NEE into its components, i.e., the fluxes related to photosynthesis and ecosystem respiration. Furthermore, there is an interest to divide the total soil respiration flux into its components, namely heterotrophic and autotrophic respiration, but this partitioning can be technically challenging. Heterotrophic respiration has been traditionally estimated with trenching, i.e., cutting of living roots in soil. However, this method is prone to errors and may not produce realistic results on the decomposition rate, since respiration is measured in the absence of living roots, while in reality roots and their exudates interact with soil microbes and thus affect the decomposition processes (Hanson et al. 2000, Subke et al. 2006, Kuzyakov et al. 2007). With isotopic methods, the different soil respiration components can be partitioned without disturbance to the intact root–soil system. The effect of living roots on decomposition rates can be estimated by utilizing the difference in isotopic signatures of the old C in soil and the fresh C derived from living biomass or artificial compounds (Baggs 2006, Hanson et al. 2000, Subke et al. 2006, Paterson et al. 2009).

A schematic CO_2 balance of a peatland ecosystem and its relationship with the methods used in this thesis are presented in Figure 1, which shows the key aboveground and belowground processes affecting the total CO_2 balance. NEE comprises gross primary production (GPP) and ecosystem respiration (ER). GPP denotes the amount of CO_2 fixed in photosynthesis, while ER derives from autotrophic respiration from the aboveground vegetation (AR_{ag}) and soil respiration (SR). SR can be divided into components by the origin of the CO_2 flux: (1) heterotrophic respiration (HR) is the decomposition of soil organic matter (SOM) and litter, originating from soil fauna and microbial organisms (fungi, bacteria and protozoans); (2) the belowground autotrophic respiration (AR_{bg}), on the other hand, is derived from roots and their associated symbiotic mycorrhizal fungi (e.g., Högberg et al. 2001, Hopkins et al. 2013). It must be noted that in reality these respiration components overlap. For example, the mycorrhizal fungi use root-derived substrates and thus contribute to both autotrophic and heterotrophic respiration (Högberg and Read 2006, Hopkins et al. 2013). The mycorrhizal respiration

has been referred to as rhizosphere respiration (RR), being composed of the respiration of mycorrhizal fungi and decomposer organisms.

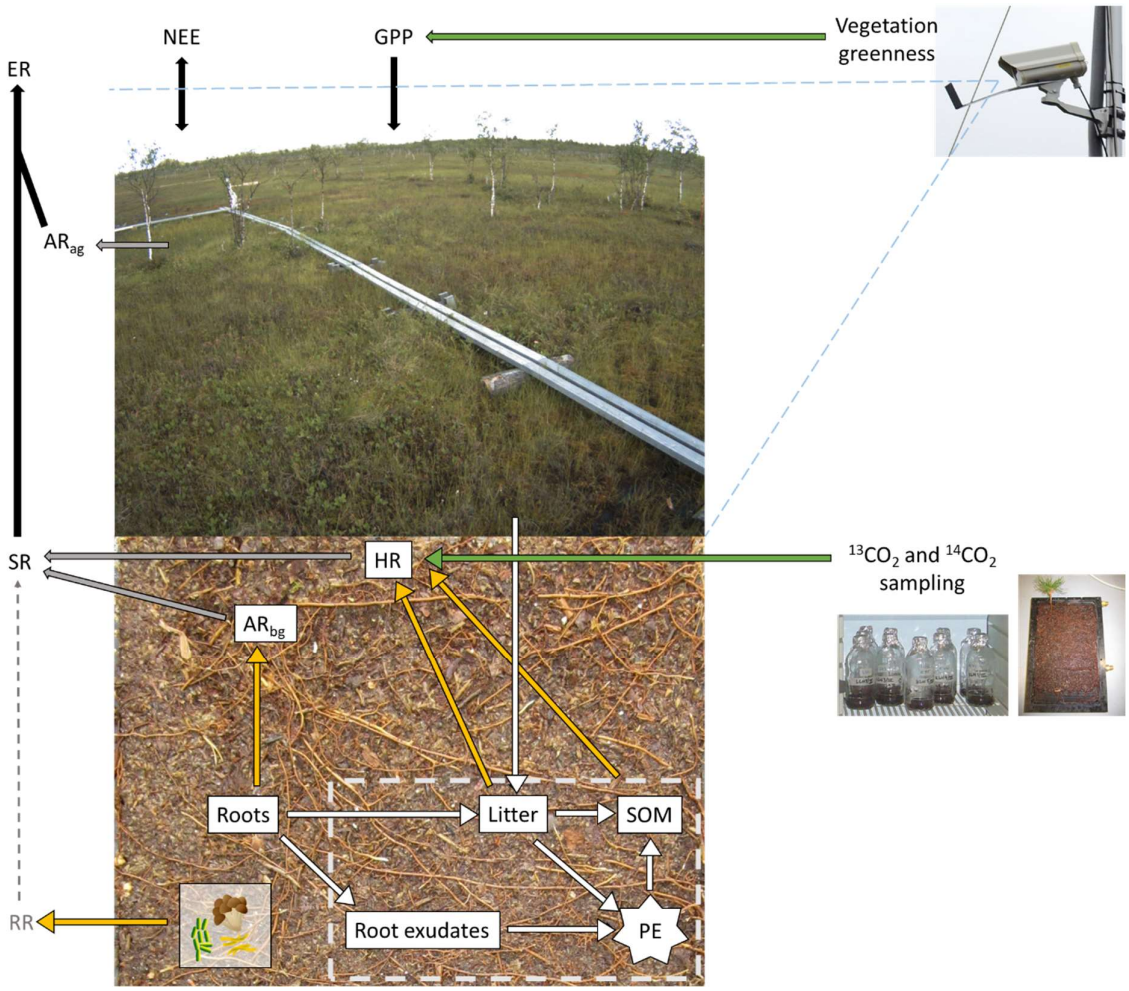

Figure 1. Schematic CO_2 balance of an ecosystem with aboveground and belowground processes (modified from Hopkins et al. (2013) and Chapin et al. (2006)) and the methods used in this thesis. The net ecosystem CO_2 exchange (NEE) consists of gross primary production (GPP) and ecosystem respiration (ER). ER can be divided into soil respiration (SR) and autotrophic respiration from aboveground vegetation (AR_{ag}), and SR can be further divided into belowground autotrophic respiration (AR_{bg}) and heterotrophic respiration (HR). Root exudates and fresh litter can affect HR through the priming effect (PE). Rhizosphere respiration (RR) is a process where root exudates are used by microorganisms (e.g., mycorrhizal fungi) and thus is not strictly autotrophic or heterotrophic. The dashed line box indicates the soil components affecting the PE. In this thesis, separate components (GPP, SR, AR_{bg}, HR) were examined with process-specific methods: digital cameras for vegetation greenness used as a proxy for GPP and laboratory-based isotope (^{13}C and ^{14}C) methods for soil respiration.

A camera or a satellite can observe the characteristics and seasonal development of aboveground vegetation, and such phenological observations can be linked to plant photosynthesis and primary production (Fig. 1). The aboveground processes affect the belowground processes and vice versa. For example, fresh C is fed to the soil system through photosynthesis, which affects the soil C

decomposition. The effect of fresh C on soil decomposition is called the priming effect (PE, Fig. 1), which refers to a change (increase or decrease) in old C decomposition after the addition of fresh C to the soil (Kuzyakov et al. 2000). In addition, soil properties affect the aboveground characteristics, such as vegetation composition and structure, and thus further the CO_2 fluxes. Furthermore, the type of soil (mineral or organic) and nutrient availability have a great impact on the respiration fluxes. Both the above- and belowground properties and characteristics of an ecosystem dictate the ecosystem–atmosphere interactions and related climatic effects. In this thesis, process-specific methods were used for studying the CO_2 fluxes originating from aboveground and belowground sources. First, greenness indices were derived from digital camera images and used for interpreting CO_2 flux measurements and evaluating satellite data, and second, isotopic methods were used for separating peat soil CO_2 respiration into its components (AR_{bg} and HR) with laboratory-based incubation and microcosm experiments.

1.2.2. Digital camera-derived greenness index describing vegetation phenology

Vegetation phenology denotes the seasonal changes in plant physiology, biomass and leaf area (Migliavacca et al. 2011, Sonnentag et al. 2011, 2012, Bauerle et al. 2012). Abiotic factors, such as precipitation, air temperature, solar radiation and water availability, are the main drivers of ecosystem functioning and vegetation phenology (Bryant and Baird 2003, Körner and Basler 2010). Due to seasonal changes in temperature, the bud burst in spring ignites photosynthesis, and again the preparation for winter dormancy in autumn appears as plant senescence. Vegetation phenology is strongly linked with plant productivity and CO_2 exchange with the atmosphere (Ahrends et al. 2009, Peichl et al. 2015, Toomey et al. 2015, Koebsch et al. 2020). Vegetation phenology also affects the surface albedo and aerodynamic roughness, thus having biophysical interactions with the climate system. The seasonal variation in vegetation phenology can be observed as substantial variation in the global atmospheric CO_2 concentration (Keeling et al. 1996).

Since the seasonal phenological phases of vegetation, i.e., different stages of plant development, are affected by abiotic factors, phenological phenomena are sensitive to changing climate (Richardson et al. 2013, Migliavacca et al. 2012). The climate warming of recent decades has advanced the start of the growing season in the boreal zone (Linkosalo et al. 2009, Delbart et al. 2008, Nordli et al. 2008, Pudas et al. 2008), and the earlier onset of growing season in turn has been observed to increase the annual C uptake of temperate and boreal forests (Berninger 1997, Black et al. 2000, Richardson et al. 2009, Park et al. 2016).

Digital cameras have proven to be a solid monitor for detecting vegetation greenness and different phenological phases (Wingate et al. 2015, Richardson et al. 2007, 2009). In contrast to satellite images, the resolution of digital images is sufficient to detect the heterogeneous microtopography and vegetation of peatlands. With digital cameras it is also possible to produce inexpensive, automated, continuous and

real-time data. A greenness index, namely the green chromatic coordinate (GCC), has been most commonly linked to vegetation greenness and CO_2 uptake of forests and peatlands (Richardson et al. 2007, 2009, Ahrends et al. 2009, Ide and Oguma 2010, Sonnentag et al. 2011, Peichl et al. 2015, Peltoniemi et al. 2018, Koebsch et al. 2020).

1.2.3. Peat soil decomposition and priming effect (PE)

Isotopic methods have been used for separating different components of the total soil CO_2 flux (Baggs 2006, Hanson et al. 2000, Subke et al. 2006, Paterson et al. 2009). These methods are based on the fact that heterotrophic soil respiration and autotrophic root and plant respiration have different isotopic signatures (Trumbore 2006). The isotopic signature ($\delta^{13}C$, ‰) denotes the ratio of stable isotopes (^{12}C and ^{13}C), and it varies approximately between -8‰ in the atmosphere and -28‰ in C3 vegetation and -26‰ in SOM (Fry 2006). The ^{14}C signature of soils and the atmosphere differ since soil respiration has an older ^{14}C signal, originating from the moment when the C atom was fixed by the plants (Hahn et al. 2006). The plants at present fix and respire CO_2 that has a ^{14}C signature similar to the atmosphere. The differences in isotopic signatures between soil and vegetation or artificial substrates enable the application of the two-pool isotope mixing model to separate the respiration derived from old and fresh C (e.g., Fry 2006, Biasi et al. 2011) and thus the partitioning of soil respiration components.

Many studies have shown that the addition of fresh substrate to soil affects the decomposition of the old organic matter in soil through the PE (e.g., Kuzyakov and Cheng 2001, Kuzyakov 2002, Subke et al. 2004). The PE plays an important role not only in soil decomposition as such (Kuzyakov et al. 2000) but also in the response of ecosystems' C dynamics to land-use and climate change (Heimann and Reichstein 2008). Since soils constitute a large C storage and the second largest CO_2 source to the atmosphere, the PE is presumed to be a key factor in the global C cycling (Bastida et al. 2019, Canadell et al. 2019). The PE can be positive or negative: when compared to the preceding level, the SOM decomposition after fresh C addition increases with positive priming and decreases with negative priming (Kuzyakov et al. 2000). A positive PE results from growing microbial activity after fresh substrate addition and the resulting increase in the decomposition of SOM (Kuzyakov et al. 2000). The addition of nutrients, such as N, further increases the microbial activity and thus amplifies the positive PE (Kuzyakov et al. 2000, Blagodatskaya and Kuzyakov 2008, Guenet et al. 2010). A negative PE has been connected to preferential substrate utilization, when soil organisms use the fresh substrate instead of the more recalcitrant old C in soil (Kuzyakov 2002, Dijkstra et al. 2013). It has also been suggested that environmental conditions and the quality of fresh C dictate the direction and magnitude of the PE (Hardie et al. 2011, Walker et al. 2016, Gavazov et al. 2018, Yan et al. 2022).

The PE has been mostly studied in mineral soils, but in recent years increasingly also in organic soils, such as peat soils. As stated above, the decomposition and nutrient availability of peat soils are likely to be affected by the C/N ratio and total N content, which may restrict the decomposition rates at more

nutrient-poor sites (Moore 2002). For organic soils, both positive PE (Hamer and Marschner 2002, Basiliko et al. 2012, Hartley et al. 2012, Bader et al. 2018, Walker et al. 2016, Mastný et al. 2021) and negative PE (Bader et al. 2018, Hardie et al. 2011, Yan et al. 2021, Mastný et al. 2021) have been reported, and there are also observations indicating no significant priming (Bader et al. 2018, Leiber-Sauheitl et al. 2015). The PE, both its magnitude and direction, still lacks understanding, but with isotopic partitioning methods it is possible to study the PE even in an intact root–soil system (Kuzyakov 2006, 2010).

1.3. Objectives and scopes

The aim of this thesis was to examine the aboveground and belowground CO_2 fluxes with process-specific methods, which support standardized flux measurements by offering additional information on the studied processes. While these methods differ widely in terms of instrumentation and experimental design, they address the same overall question as there is a strong link between the aboveground plant development and the belowground decomposition processes.

In Papers I and II, the seasonal development and greenness of vegetation were observed for different ecosystems with phenology cameras. The vegetation phenology data were analyzed together with CO_2 flux measurements and meteorological data and compared with satellite-derived greenness data. The combined aims of these phenology camera studies were (1) to evaluate the digital repeat photography and satellites as a method for monitoring vegetation greenness and development, (2) to examine the differences in vegetation dynamics between two adjacent but contrasting ecosystems, three different pristine peatlands and different plant communities within a peatland ecosystem and (3) to assess the utility of phenology camera data in the interpretation of concurrent CO_2 flux measurements.

In Papers III and IV, the soil CO_2 fluxes and PE in two forestry-drained peatlands were studied in the laboratory with isotope techniques. The combined aims of these PE studies were (1) to examine the differences in the basal peat soil respiration between two peat soils and (2) to study the magnitude and direction of the PE of peat soils with different nutrient status after addition of fresh C, and to further study whether the addition of supplementary nutrients affects the peat respiration and PE and (3) to analyze whether the peat respiration rates and PE could explain the observed difference in C balance between the sites.

2. Material and methods

2.1. Study sites

The phenology cameras employed in Paper I and II are located in northern Finland at three pristine state aapa mire peatlands: Halssiaapa, Lompolojänkkä and Kaamanen. The study sites of Papers III and IV, forestry-drained peatlands Lettosuo and Kalevansuo, are located in southern Finland (Fig. 2).

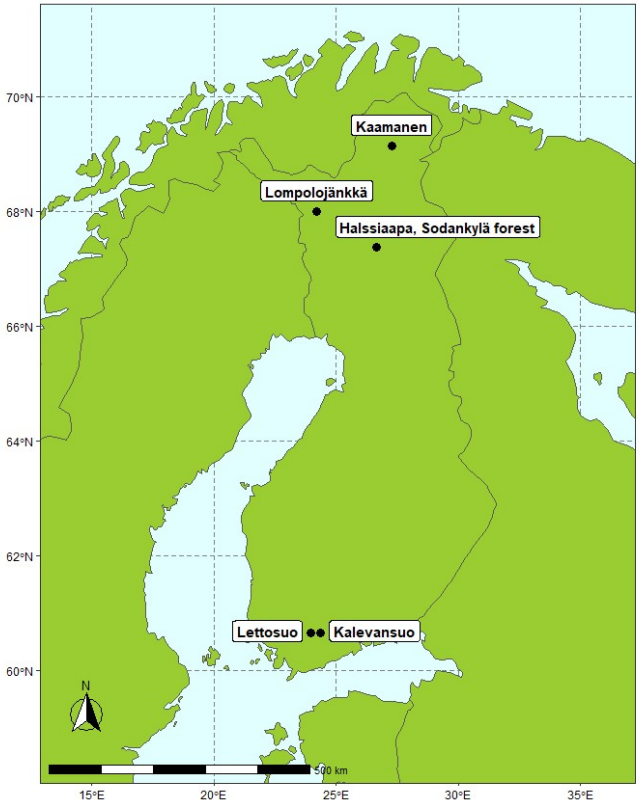

Figure 2. Location of the study sites (Papers I, II, III and IV)

Table 1. General properties of the study sites (Papers I, II, III and IV)

	Coordinates	Altitude (m.a.s.l.)	Ecosystem type	Mean temperature (°C)	Mean annual precipitation (mm)	Soil type	Mean vegetation height (m)
Halssiaapa	N67°22.117' E26°39.244'	180	Fen	0.3	542	Peat	0.4
Lompolojänkkä	N67°59.835', E24°12.546'	269	Fen	0.4	644	Peat	0.4
Kaamanen	N69°8.435', E27°16.189	155	Fen	0.1	467	Peat	0.3
Sodankylä forest	N67°21.708', E26°38.29'	179	Scots pine forest	0.3	542	Sandy pozol	12
Lettosuo	N60°38.510' E23°57.583'	111	Forestry-drained peatland	5.3	640	Peat	20
Kalevansuo	N60°38.81' E24°21.37'	123	Forestry-drained peatland	4.6	660	Peat	18

Halssiaapa, located in Sodankylä, about 100 km north of the Arctic circle, is the southernmost of the sites (Table 1) and studied in Papers I and II. The vegetation in this mesotrophic fen varies between the higher and drier strings and the wetter and lower flarks. The tree stand is sparse and low, mostly consisting of *Betula pubescens* and few small *Pinus sylvestris* trees. The ground vegetation is dominated by shrubs (*Andromeda polifolia, Betula nana, Vaccinium oxycoccos*) growing mostly on strings, while the flarks are covered by sedges and herbs (*Carex* spp*., Menyanthes trifoliata*) and *Sphagnum* mosses.

Lompolojänkkä is a nutrient-rich sedge fen located in the Pallas area in north-western Finland (Table 1). Of the study sites in Paper II, this is the richest in nutrients, which is reflected in the rich vegetation. The vegetation is mainly dominated by *Betula nana, Menyanthes trifoliata, Salix lapponum* and *Carex* spp. with *Sphagnum* and brown mosses (Aurela et al. 2009).

Kaamanen is the northern most of the sites studied in Paper II (Table 1). It is located within the northern boreal vegetation zone, but the regional climate is already subarctic (Aurela et al. 1998). Vegetation is distributed to wet flarks and higher strings. The vegetation on the strings consists mainly of ombrotrophic species, such as forest mosses and Ericales (Maanavilja et al. 2011). *Sphagnum*-mosses, sedges, *Betula nana* and *Andromeda polifolia* dominate the margins of the strings. The flarks have mesoeutrophic vegetation with brown mosses and sedges (Maanavilja et al. 2011).

In Paper I, two adjacent but different ecosystems, namely a peatland and a Scots pine forest, were studied. The peatland site was Halssiaapa, described above. The Scots pine site (N67°21.708', E26°38.29', 179 m a.s.l.) is located 1 km south-west of Halssiaapa. The site has fluvial sandy podzol soil. The dominant tree height is 13 m and the tree density is 2100 ha^{-1}. The age of the trees within the camera scope was about 50 yr during the time of the study. A single-sided leaf area index (LAI) of 1.2 has been estimated for the stand based on a forest inventory. The sparse ground vegetation consisted of lichens (73%), mosses (12%) and ericaceous shrubs (15%).

The study sites of Papers III and IV were located in Southern Finland about 20 km apart (Table 1). Both sites were drained for forestry in the beginning of the 1970s, about 40 yr before these studies. The sites differed in nutrient status, and the nutrient-rich (NR) site (Lettosuo, Tammela municipality) is a drained herb-rich, tall sedge, birch-pine fen, while the nutrient-poor (NP) site (Kalevansuo, Loppi municipality) is a dwarf-shrub pine bog. At the time of the peat sampling, the main tree species at the NR site were Scots pine (*Pinus sylvestris*) and downy birch (*Betula pubescens*), with an understorey layer of Norway spruce (*Picea abies*). At the NP site, Scots pine dominated the tree stand with an understorey of downy birch. The tree stand was taller and denser at the NR site (volume 220 m^3 ha^{-1}, density 2220 trees ha^{-1}) compared to the NP site (volume 130 m^3 ha^{-1}, density 750 trees ha^{-1}). The forest floor vegetation was sparser and smaller at the NR site, mostly consisting of forest shrubs and mosses. The forest floor vegetation at the NP site was a combination of forest and mire dwarf shrubs.

The average water table level and the depth of the peat layer of the study sites in Papers III and IV were of the same magnitude, -50 cm and 2.6 m at the NR site and -40 cm and 3.0 m at the NP site, respectively (Stén 1998, Lohila et al. 2011). The *in situ* soil C/N ratio and nutrient analysis showed that the C/N ratio at depths of 0–10 and 10–20 cm was 25.2 ± 3.0 and 23.9 ± 1.5 (±SD), respectively, at the NR site (Korkiakoski et al. 2017) and 34.1 ± 1.6 and 37.9 ± 1.4 (±SD), respectively, in the NP peat soil (Lohila et al. 2011). The surface peat nitrate (NO_3^-) and ammonium (NH_4^+) concentrations were significantly higher in the NR peat, 20.5 ± 3.0 mg NO_3^--N kg DW^{-1} and 39.4 ± 10.1 mg NH_4^+-N kg DW^{-1} (±SD), than in the NP peat, 1.1 ± 1.1 mg NO_3^- -N kg DW^{-1} and 6.2 ± 3.2 mg NH_4^+-N kg DW^{-1} (±SD) (measured in August 2010, M. Pihlatie, personal communication). The ash content, pH and bulk density were lower at the NP site. Some of the element concentrations were higher at the NR site, including copper (Cu), manganese (Mn), phosphorus (P), aluminium (Al), iron (Fe) and calcium (Ca), while some were higher at the NP site, including potassium (K), magnesium (Mg), zinc (Zn), sodium (Na), lead (Pb), nickel (Ni), boron (B) and cadmium (Cd) (Lohila et al. 2011, unpublished data). In general, the trace element concentrations at the sites were about the same with the exception of Fe, for which a six-fold concentration was found at the NR site compared to the NP site. This difference most probably reflects the origin of the NR site as a fen and thus is a result of hydrological features.

It has been previously verified, that these two forestry-drained peatlands have a different C balance. EC and related tree biomass measurements show that the soil in the NP site is a small sink of C and the NR site is releasing C (Lohila et al. 2011, Minkkinen et al. 2018, Kasimir et al. 2021, Korkiakoski et al. 2023). It was hypothesized that these differences in the C balance could be explained by the differences in soil respiration rates and particularly by the PE.

2.2. Studies on the aboveground vegetation greenness (Papers I and II)

In Papers I and II, the greenness indices derived from phenology camera images were combined with ecosystem-scale CO_2 flux, air temperature and satellite-derived greenness data. Phenology cameras were mounted within three pristine peatlands and a Scots pine forest.

2.2.1. Digital camera setups

StarDot Netcam SC 5 digital cameras were used for phenology monitoring. The cameras were weather proofed and connected to line current and a web server (Fig. 3). The images with a 2592 × 1944 resolution in the 8-bit JPEG format were stored automatically every 30 minutes during the daylight hours and transferred to the server. At peatland sites (Papers I and II), the cameras were facing north in depression angles of 18° at 2 m height at Halssiaapa, 10° at 3-m height at Lompolojänkkä and 10° at 3.5-m height at Kaamanen. The cameras were observing mostly ground vegetation, but also some trees and skyline were visible. All the cameras had the same image quality setting for saturation, contrast and colour balance. At the forest site (Paper I), the cameras were located at two different heights: 29 m

('canopy camera') and 13 m ('crown camera'). The viewing angle was 45° for the canopy camera, and the crown camera was positioned nearly horizontally. The camera view of the canopy camera showed the forest canopy and general landscape, while the crown camera observed individual trees for a more accurate detection of phenological development.

Figure 3. Examples of the camera setups at Kaamanen (left) and Halssiaapa (right). Photos: Courtesy of FMI.

2.2.2. Image processing

For Papers I and II, the digital images were analyzed with the FMIPROT software, an image processing tool for phenological and meteorological observations (Tanis et al. 2018). The program calculates the colour fractions of red, green and blue channels in the image pixels. From this information, the GCC is calculated as:

$$GCC = \frac{\Sigma G}{\Sigma R+\Sigma G+\Sigma B} \quad (1)$$

where ΣG, ΣR, ΣB are the sums of green, red and blue channel indices within the image.

We used image data obtained only after the snowmelt, which usually occurs in May at all sites, since visible snow in the images causes overexposure.

2.2.3. Regions of interest (ROIs)

With the FMIPROT it is possible to crop Regions of Interest (ROIs) within an image. This makes it possible to analyze a subarea of the image, for example, different plant communities or even individual plant species. In Papers I and II, both general ROIs and more specific ROIs limited to distinctly identifiable plant communities were chosen for the analysis.

2.2.4. Testing of the digital camera setup

In Paper I, the stability of the image colour channels was studied by installing grey reference plates within the camera view. The aim was to examine if changing conditions, such as changes in solar radiation, affect the colour balance of the images of reference plates, which should not show any seasonality (Petach et al. 2014). The reference plate was painted with Tikkurila grey/1948 colour, where the red, green and blue colour components (RGB) were equal (R = G = B = 95). The mean diurnal GCC cycle was then calculated for the reference plate throughout the year and the stability of reference images was analyzed for different months and hours of the day.

The effect of cloudiness on the GCC data was tested with the data collected in July 2014, when the growing season peaked and, in addition, an equal number of sunny and cloudy days was observed. The images were classified by the observation of cloudiness (from clear sky to completely cloudy, CL = 0–8) to two groups, sunny (CL = 0–1) and cloudy (CL = 7–8). The daily (11.00–15.00) mean GCC of these groups was then compared. The effect of sun angle on the images was tested by comparing the mean minimum and maximum GCC for the sunny and cloudy days within the daytime window.

To test the effect of ROI selection on GCC, four different and clearly identifiable vegetation types were chosen from the fen site, in addition to the more general ROI including multiple vegetation types. The dominant vegetation within those ROIs were (1) bog-rosemary (*Andromeda polifolia)* and other shrubs, (2) sedges (*Carex* spp.*)* and *Sphagnum* mosses, (3) big-leafed bogbean (*Menyanthes trifoliate)* and (4) downy birch (*Betula pubescens).*

2.2.5. Temperature dependency calculations

In Paper II, the growing degree day sum (GDDS) was calculated as the cumulative sum of the daily average temperatures that exceeded 5 °C, subtracting the base value of 5 °C. When the daily mean temperature had remained over 5 °C for ten days, the growing season was accounted to start. In addition, short-term changes in GCC were examined by calculating the mean three-day difference, i.e., by defining $\Delta GCC = GCC(day_t) - GCC(day_{t+3})$. ΔGCC was divided into three classes by temperature (< 5 °C, 5–10 °C and > 10 °C) calculated as a two-day average (day_t and day_{t+1}).

2.2.6. Fitting of the GCC and daily maximum GPP cycles

To illustrate the seasonal GCC cycle, a double hyperbolic tangent function was fitted in Paper II to both camera- and satellite-derived GCC time series (Meroni et al. 2014, Vrieling et al. 2018):

$$GCC(t) = a_0 + a_1 \frac{\tanh((t-a_2)a_3)+1}{2} + a_4 \frac{\tanh((t-a_5)a_6)+1}{2} - a_4 \quad (2)$$

where t is time, a_0 is the minimum GCC in the beginning of the growing season, a_1 (a_4) is the difference between the maximum GCC and minimum GCC, a_2 (a_5) is the inflection point in GCC development, and a_3 (a_6) controls the slope at the inflection point in GCC development during the first (second) half of the growing season. This function was also fitted to the daily maximum GPP data.

The fit for camera- and satellite-derived data was fixed to start on 1 May with a fixed GCC value. This GCC value was averaged for each site from the annual minima right after the snowmelt. Similarly, the end point of the fit was fixed to 31 October, with the average of the annual GCC minima at the end of the growing season. The same procedure was applied to the daily maximum GPP data. The fitted GCC functions were used to define parameters describing different phenological phases and vegetation development. The start of season (SOS25), calculated as 25% of the GCC difference between the maximum and 1 May, the maximum GCC (MAX) and the end of season (EOS25), calculated as 25% of the GCC difference between 30 October and the maximum, were used as descriptive parameters for comparison between the camera- and satellite-derived data.

2.2.7. Autocorrelation between GCC and daily maximum GPP data

Autocorrelation in the residuals of the regression between GCC and the daily maximum GPP was tested with the Durbin–Watson test. Autocorrelation was taken into account by regressing the first differences of the data, i.e., by applying the transformation $x'_t = x_t - x_{t-1}$, where x_t and x_{t-1} are consecutive observations.

2.2.8. Ecosystem scale CO_2 exchange and meteorological measurements

The CO_2 exchange between ecosystems and the atmosphere was measured with the micrometeorological EC method at all sites (Papers I and II). The EC method is based on determining the covariance between the high-frequency fluctuations in vertical wind speed and CO_2 mixing ratio (Baldocchi 2003). The EC measurement systems included USA-1 (METEK GmbH) three-axis sonic anemometers/ thermometers and closed-path LI-7000 (Li-Cor., Inc., Lincoln, NE, USA) CO_2/H_2O gas analyzers. In addition, air temperature, photosynthetic photon flux density (PPFD) and water table level were measured at the sites. Cloudiness data were obtained from the observatory in Sodankylä. For more detailed information about the measurement systems and data processing, see Aurela et al. (2009).

EC measures the net ecosystem exchange which, as depicted in Figure 1, consists of gross photosynthetic production and ecosystem respiration. The daily maximum GPP (GPP_{max}, denoted by GPI in Paper I) expresses the maximal photosynthetic activity in optimal radiation conditions and is here calculated as the difference between the daily average of the daytime (PPFD > 600 μmol m^{-2} s^{-1}) and night-time (PPFD < 20 μmol m^{-2} s^{-1}) NEE.

2.2.9. Satellite (Sentinel-2) data

In Paper II the GCC was also derived from the Sentinel-2 data collected in 2016–2019. The satellite data consisted of bottom-of-atmosphere products (Level-2A) which were atmospherically corrected. The bands that were used were B2 (blue, 490 nm), B3 (green, 560 nm) and B4 (red, 665 nm). The spatial resolution was 10 m. The Sentinel Scientific Data Hub (https://scihub.copernicus.eu) was used for downloading the products.

If there was no Level-2A product available for a certain day, the Level-1C product was processed with the Sen2Cor software (version 2.8) to correspond with the Level-2A product. The cloudy, cloud-shadowed and snowy satellite images were filtered with the scene classification data (SCL Band) available in the Level-2A products. Although the satellite data were available at least every other day, the filtering decreased the number of valid images.

The GCC from the satellite images was calculated as an average from the multiple ROIs within each site. The ROIs were chosen to represent different vegetation types and microtopography. Due to the difference in spatial resolution of the images, the ROIs were not the same as in the camera images.

2.3. Studies on the belowground CO_2 fluxes (Papers III and IV)

The belowground decomposition of the old SOM was studied in Papers III and IV with natural abundance and ^{13}C-labelling experiments. The peat soil for both studies was collected from two sites with different nutrient status. The sites were defined as nutrient-rich (NR) and nutrient-poor (NP) peatlands based on their original peatland type.

2.3.1. Soil sampling

The peat for both incubation experiments (Papers III and IV) was collected from the sites from four locations within a distance of 100 m. From each location, three peat core samples were collected from an area of about 1 m^2. In total, 12 peat core samples with two depths were collected from both sites. For the natural abundance study, the core samples included two depths: 10–20 cm (younger surface peat) and 40–60 cm (older, deep peat). For the ^{13}C-labelling study the peat samples were taken just below the litter and humus layer. All the peat samples were homogenized and roots were removed. For the natural abundance experiment the peat was incubated for six months at 5 °C before the experiment. During the

long incubation period, the easily decomposable material was decomposed. For the ^{13}C-labelling study the peat was stored in cold for two weeks before the experiment started.

2.3.2. Methods of the natural abundance study of ^{14}C

For the experiment of natural abundance of ^{14}C (Paper III) a 6-month laboratory study was established. Pine seedlings were planted in microcosm systems, as described by Pumpanen et al. (2009). The microcosm was built from a compartment for the soil and roots and a transparent lid (Fig. 4). The soil compartment had carved channels for air transport and tube connection holes. The size of the microcosm was 200 mm × 300 mm. A 5-mm layer of peat was spread to 56 microcosms (28 with deep peat and 28 with surface peat). To 32 of the microcosms a 2-month-old seedling (*Pinus sylvestris*) was planted while 24 microcosm remained as bare peat controls. Half of these microcosms represented the NR site and half the NP site. The microcosms were set in a greenhouse in insulated boxes (Fig. 4). The boxes were cooled by circulating water cooled to 10 °C by a Lauda cooling system (model RM, Lauda-Königshofen, Germany) at the bottom. The soil and root compartments were covered to block the light access to the roots. The light in the greenhouse was turned on for 18 h per day with a light intensity set approximately to 300 µmol m^{-2} s^{-1}. In addition, the temperature in the greenhouse was controlled and recorded.

Figure 4. Example of a microcosm system with peat and a pine seedling (left) and setup for the microcosm systems in a greenhouse with the Lauda cooling system (right). Photos: Maiju Linkosalmi

The planted seedlings were germinated from seeds collected nearby the study sites. The germination was conducted in sterile conditions as described by Heinonsalo et al. (2001). To ensure the presence of natural microflora, the seedlings were also inoculated with a solution extracted from the peat soil of the study sites. Later, when the seedlings were observed to suffer from nutrition deficiency, they were fertilized with PK fertilization extract (7% P, 11.3% K and 0.23% Fe). In addition, the control microcosms were fertilized to preserve the difference in the nutrient content between different peat

soils. All the microcosms were watered every second day with distilled water and weighed before and after the watering to keep the moisture content stable.

The CO_2 fluxes (respiration of peat with and without a seedling and seedling photosynthesis) were measured from 3-, 5-, 6- and 8-month-old seedlings. Compressed air was led through the microcosm, and the difference between incoming and outgoing concentrations of CO_2 and water vapour was analyzed with a LI-7000 gas analyzer (LI-COR Inc., Lincoln, NE, USA). Photosynthesis was measured with an attachable transparent chamber, and the gas analysis was conducted as described above. The PPFD was set approximately to 450 µmol m^{-2} s^{-1}. The procedure is described more precisely by Pumpanen et al. (2009).

According to the percent modern carbon (pMC) analyses, conducted in advance, the surface peat at both sites is younger than the deeper peat; at the NR site, pMC was 100.9% and 78.4%, in the surface and deep peat and at the NP site 92.3% and 67.7%, respectively. Thus, the difference in isotopic composition between the deeper peat and surface peat or living plants was sufficient for a reliable application of the mixing model (Biasi et al. 2011). Molecular sieves were used for collecting $^{14}CO_2$ samples from the respiration of bare peat and peat with roots (Hämäläinen et al. 2010, Palonen and Oinonen 2013). After the experiment, all the components (peat, root, seedlings) were separated and weighed. The samples were dried to determine the dry weight and moisture content.

2.3.3. Methods of the ^{13}C-labelling study

The ^{13}C-labelling experiment (Paper IV) included 120 peat sample bottles (60 per site), with approximately 20 g of peat in each bottle, which were incubated at 15 °C during the experiment. Half of the peat samples were labelled with 500 µg g DW^{-1} of ^{13}C-glucose. To examine the effect of nutrients on decomposition, 30 labelled and 30 non-labelled samples were fertilized with a solution containing N, P and K. 30 peat samples were control samples without nutrients and ^{13}C-glucose. The treatments for both sites were sorted to three batches, each batch consisting of 20 samples (5 control samples, 5 samples with nutrient addition, 5 samples with ^{13}C-glucose addition and 5 samples with nutrient and ^{13}C-glucose addition). The CO_2 and $^{13}CO_2$ emissions were measured from one batch throughout the experiment. The additional analyses (C, N, NO_3^-, microbial biomass C) were conducted three times during the experiment for each batch.

The CO_2 production rates were analyzed by taking syringe samples from closed, air tight sample bottles first after 30 min and again after 5 h after closure of the bottles. The CO_2 concentration in syringe samples was analyzed with a gas chromatograph (Hewlett Packard 5890 Series II). The $^{13}CO_2$ -samples were taken after 5 h with vacuum degassed vials, and the samples were analyzed with an IRMS (Isotope Ratio Mass Spectrometer). This was repeated during the first four days of the experiment, then every second day and lastly after three days.

The concentrations of NO_3^- were determined with an ion chromatograph (Dionex DX-120) from extractions of fresh peat. The amount of microbial biomass C in the peat samples was determined with chloroform fumigation extraction. The concentrations of dissolved organic C (DOC) and dissolved N (DN) contents were analyzed with a Shimadzu (Japan) analyzer from fumigated and non-fumigated extracts. The isotopic ratio was also determined from the fumigated and non-fumigated samples with the IRMS.

2.3.4. Two-pool mixing model

In Papers III and IV, the observed respiration fluxes were partitioned with the two-pool mixing model (Fry 2006, Hahn et al. 2006, Biasi et al. 2011). In Paper III, the ^{14}C dating results, i.e., the pMC values, were used for the calculation of the fraction of peat-derived respiration:

$$f_{peat} = \frac{pMC_{mix} - pMC_{modern}}{pMC_{bare} - pM_{modern}} \quad (3)$$

where pMC_{mix} denotes the $^{14}CO_2$ signal from peat and seedling respiration, pMC_{bare} is the ^{14}C signal of CO_2 from bare peat respiration, and pMC_{modern} stands for the modern C pMC (here we use the value of 105%). The f_{peat} fraction was calculated for both the NR and NP deep peat treatments.

In Paper IV, which reports the ^{13}C-labelling study, the fraction of peat-derived respiration (f_{peat}) was calculated from the analyzed $\delta^{13}C$ results as:

$$f_{peat} = \frac{\delta^{13}C_l - \delta^{13}C_n}{\delta^{13}C_g - \delta^{13}C_n} \quad (4)$$

where $\delta^{13}C_l$ denotes the $\delta^{13}C$-value of labelled peat, $\delta^{13}C_n$ is the $\delta^{13}C$-value of non-labelled peat, and $\delta^{13}C_g$ is the $\delta^{13}C$-value of the added ^{13}C-glucose. The f_{peat} fraction was calculated for both the NR and NP peat treatments.

3. Results

3.1. Studies on the aboveground vegetation greenness (Papers I and II)

The digital camera-derived greenness index was determined for different sites and measurement years, and combined with CO_2 measurements, air temperature and satellite data in Papers I and II.

3.1.1. Testing of the digital camera setup

In Paper I, the experimental setup for phenological monitoring was tested by analysing the grey reference plate data.

The periods with sufficient light levels for the GCC analysis were determined from the daily data, which showed that GCC remained stable from March to October (Paper I: Fig. 4). During winter months, the solar radiation is low in northern Finland, which decreased the GCC levels and increased the short-term variance of GCC. In the night-time GCC data, the variance was high all year round, even though in high latitudes the summer nights are not completely dark. The daytime period for the final GCC analysis was limited to 11.00–15.00 (UTC+2).

The examination of the effect of cloudiness on the GCC data showed no significant difference in the mean GCC between sunny and cloudy conditions (Paper I: Fig. 4). The significance of solar angle was tested by comparing GCC data obtained before and after noon and no difference was found.

To test the effect of ROI selection on GCC, four different and clearly identifiable vegetation types were chosen from the fen site, in addition to the more general ROI including multiple vegetation types. The GCC of these different ROIs showed significant differences in their seasonal cycle, such as in the timing of phenological phases and the maximum GCC values (Paper I: Fig. 5). The downy birch-dominated ROI showed the fastest growth onset in spring, and the ROI with big-leafed bogbean showed the highest maximum GCC. At the forest site, the effect of ROI selection was tested by subjectively selecting three separate ROIs from the general canopy view. There were no differences in the daily mean GCC values of these ROIs.

The GCC values of forest were lower when determined from the canopy camera images than from the crown camera images (Paper I: Fig. 6). Most probably, this was due to the different viewing angles of these cameras and the different distances between the camera lenses and the objects. In addition, soil and snow may be visible in the background in the canopy images, which affects the GCC observation. For further analysis, only the crown camera images were used.

3.1.2. Development of GCC and GPP_{max} at peatland sites

In Paper I, the vegetation greenness was derived from digital images of the Halssiaapa fen for two growing seasons, 2014 and 2015. For Paper II, the digital camera setup observing peatland vegetation was extended to cover also two other pristine peatlands and five growing seasons (2015–2019). The images from all the study sites visually show the seasonal development of vegetation greenness: spring development, greening, peak season and senescence (Fig. 5). The development of GCC was clear at all sites: as the vegetation starts to develop in the spring after snowmelt, also the GCC starts to increase (Fig. 6). The snowmelt occurs in northern peatlands on average in May. The period between snowmelt and vegetation growth onset is visible in the GCC data as a decrease due to the moist and dark soil (data not shown).

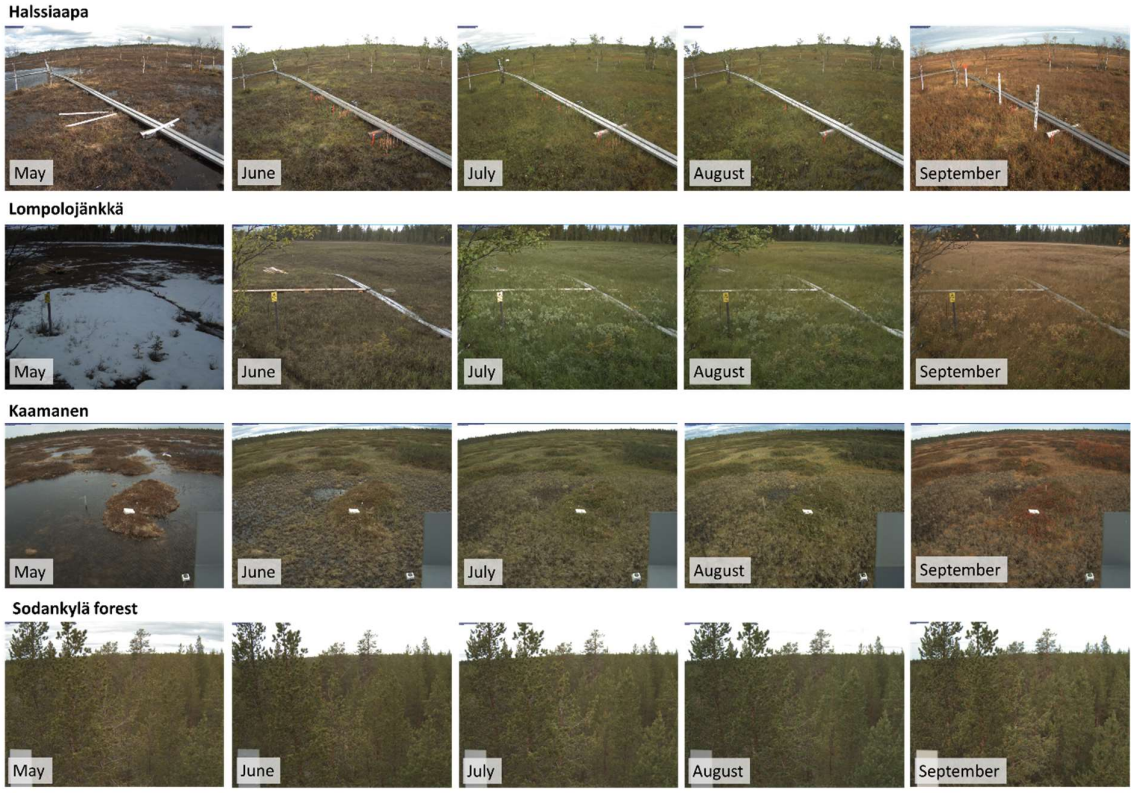

Figure 5. Seasonal development of vegetation and surface water from May to September 2015 at the Halssiaapa, Lompolojänkkä and Kaamanen fens, and at the forest site in Sodankylä. The pictures were taken on the 15th of each month. Figure modified from Paper II.

The GCC data over the five measurement years 2015–2019 demonstrated that GCC was systematically highest at Lompolojänkkä ($p < 0.05$) (Fig. 6). In addition, the difference between Halssiaapa and other sites was significant in mean growing season GCC values in 2017, 2018 and 2019. At Lompolojänkkä and Kaamanen the maximum GCC was observed in 2017 and at Halssiaapa in 2016.

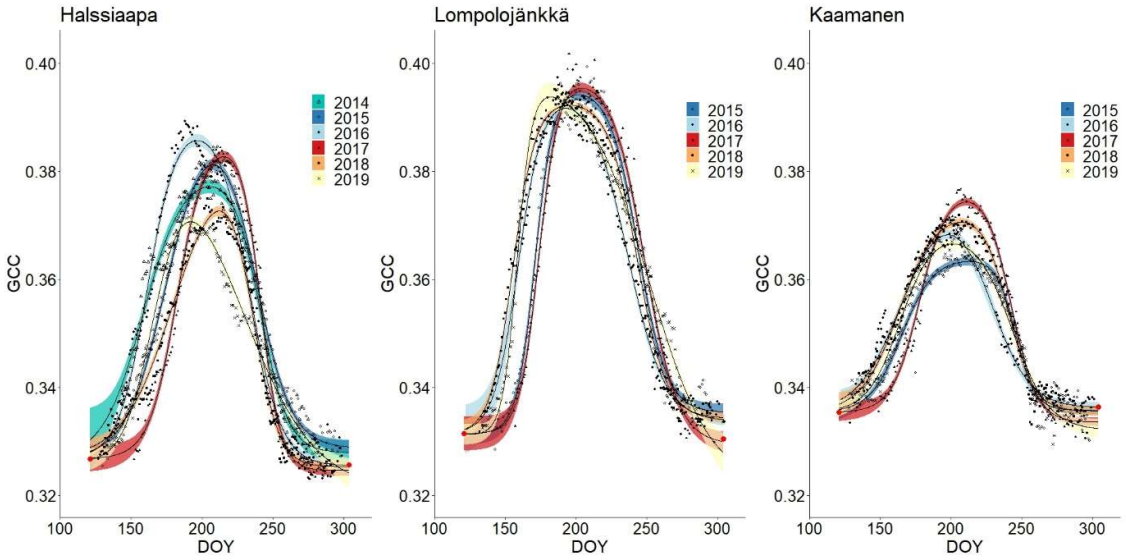

Figure 6. Development of GCC during six growing seasons (2014–2019) at Halssiaapa, and five growing seasons (2015–2019) at Lompolojänkkä and Kaamanen. The different symbols denote different years and the bands with different colours denote the 95% confidence intervals of the fitted hyperbolic tangent function. The red dots indicate the fixed start and end days defined for the fitting. Figure modified from Paper II.

The differences in GCC among different plant communities were examined in Paper II. The differences were significant at all sites ($p < 0.05$), with the exception of 2017 at Halssiaapa and Kaamanen. The GCC of birch species differed at all sites significantly from the GCC of other plant communities. Comparisons of the maximum GCC values of different plant communities showed that the annuals and woody plants with bigger leaves produced a higher GCC than *Carex* species and shrubs.

The seasonal pattern throughout the growing seasons was similar in the GCC and GPP_{max} data (Figs. 6 and 7). No differences in the GPP_{max} were observed among the sites in 2015, but in 2016 and 2019 a significant difference between Kaamanen and the other two sites was found, and in 2017 and 2018 between Lompolojänkkä and Kaamanen. A linear relationship existed between GCC and the GPP_{max}, but also a significant autocorrelation in the model residuals was found in Paper II (Paper II: Table 5). After taking the autocorrelation into account, the coefficient of determination was generally reduced to close to zero. Even though some short periods showed correlated variation in GCC and the GPP_{max} (Papers I and II), it was concluded that most of the common variation was explained by the common seasonal cycle.

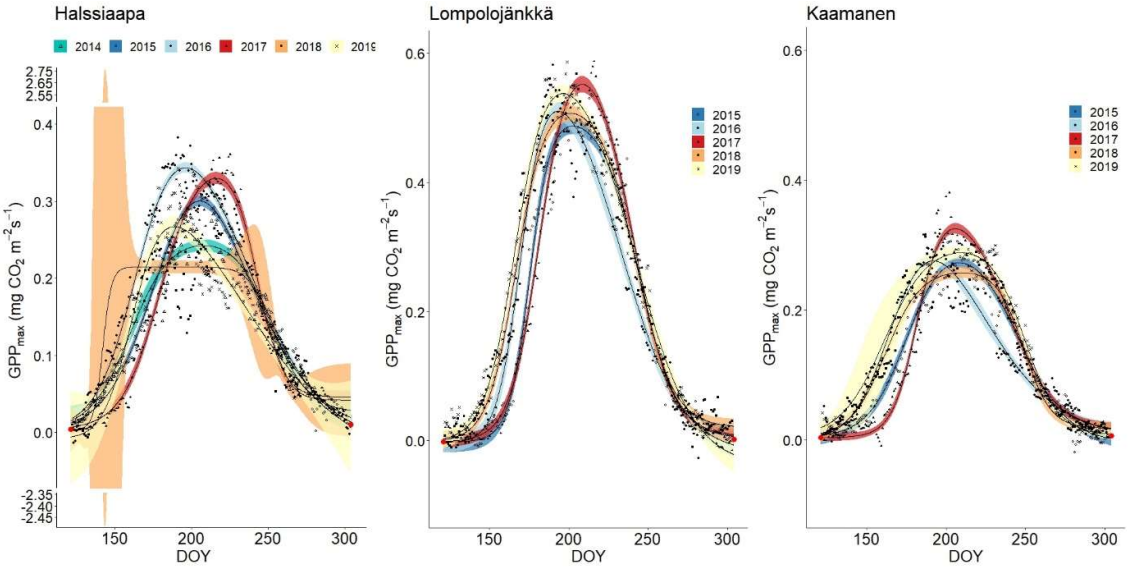

Figure 7. Development of the daily maximum GPP (GPP_{max}) during six growing seasons (2014–2019) at Halssiaapa, and five growing seasons (2015–2019) at Lompolojänkkä and Kaamanen. The different symbols denote different years and the bands with different colours denote the 95% confidence intervals of the fitted hyperbolic tangent function. The red dots indicate the fixed start and end days defined for the fitting. Figure modified from Paper II.

3.1.3. GCC and GPP_{max} at forest site during two growing seasons

In Paper I, GCC was also determined for a pine forest site located close to the Halssiaapa fen. The meteorological conditions were similar due to the proximity of the sites. As the pine forest site has evergreen vegetation, photosynthesis can start quickly as soon as air temperature reaches a sufficiently high level. For example, the effect of the few warm days in the beginning of May 2015 was visible in the GCC of the forest, but not in the GPP_{max} at the fen whose vegetation was not yet active (Paper I: Figs. 7 and 8). In addition, due to this warm period, the growing season in 2015 started earlier than in 2014 at the forest site, but this was not observed at the fen site. As also observed for the fen, the warm period in May–June 2014 enhanced the forest growth and by mid-June the GPP_{max} and GCC exceeded the corresponding levels in 2015. However, the cold period later in June 2014 decreased both the CO_2 uptake and GCC at both sites. The reduction in GCC was more distinct for the forest than for the fen.

3.1.4. Temperature dependence of GCC and GPP_{max}

The GCC and GPP_{max} data in Paper I show that due to warm spells the fen vegetation developed rapidly during May–June 2014 and thus the growing season development was faster in 2014 than in 2015 (Paper I: Fig. 7). The earlier onset in 2014 also resulted in an earlier occurrence of the maximum GCC. Both GCC and the GPP_{max} show a stabilization and reduction in late June 2014, which occurred at the same time as a colder period. The maximum GCC was similar in these two years, and so was the rate of GCC decline during August and September. In 2014, a warm period took place in mid-September, which

most likely was the explanation for the slightly higher GCC values observed. When the daily temperatures dropped below 0 °C in October, GCC decreased close to the values observed before the growing season start.

Consistently, warmer conditions in spring and an earlier snowmelt led to an earlier green-up of the vegetation. The late snowmelt in 2017 delayed the start of GCC development and photosynthesis compared to the other study years (Paper II: Figs. 7–9). However, no connection was found in Paper II between the timing of growing season start and the maximum GCC or GPP_{max} at Lompolojänkkä or Kaamanen. At Halssiaapa, the earliest growing season start, the maximum value and the earliest timing of GCC and the GPP_{max} all happened in 2016, i.e., during the same year (Paper II: Table 3).

In Paper II, the temperature dependence of GCC was studied by creating a normalized cumulative GCC and GDDS for all the sites and growing seasons. These results showed that the increase of GCC started later than the accumulation of GDDS. The cold spring and later melting snow cover in 2017 delayed both the GDDS and GCC compared to the other growing seasons studied (Paper II: Fig. 5). Although the start of the growing season started later in that year, the vegetation was able to reach its typical development rate, and the highest summer maximum GCC was observed at Lompolojänkkä and Kaamanen (Paper II: Table 3).

The year 2018 was the warmest of the study years 2015–2019 at all the sites. At Halssiaapa, drought with a substantial water table drop was observed in July 2018, and again in July and August 2019, and it was reflected in both GCC and the GPP_{max} (Paper II: Fig. 7). The drought periods also affected the WTD and GCC at Kaamanen, but not at Lompolojänkkä.

The short-term GCC change (ΔGCC), indicative of vegetation development within different temperature classes, depended on both the month and temperature range (Paper II: Fig. 6). In May, the mean ΔGCC was substantially smaller for temperatures below than above 5 °C. In the lowest temperature class (< 5 °C), no significant differences were found among the sites during any month. The vegetation growth was found to benefit from lower temperatures at Lompolojänkkä, and it was overall larger than at the other sites. In June, the temperature limit for positive ΔGCC was over 10 °C at Halssiaapa, while at Lompolojänkkä this limit was lower and at Kaamanen the mean ΔGCC of June was similar in all temperature classes. The mean ΔGCC started to stabilize during July, but at Kaamanen a significant positive change was observed for temperatures between 5 and 10 °C, and at Halssiaapa for temperatures over 10 °C. The mean ΔGCC was negative due to senescence in August and September. The ΔGCC indicator was calculated also separately for different plant communities, and the results showed that *Betula* spp. started a rapid growth in May at all sites, but already in June the ΔGCC of birches was lower than in other plant communities. As in the spatially averaged ΔGCC data, the highest plant community-specific ΔGCC values were found at Lompolojänkkä.

3.1.5. GCC derived from satellite data

The GCC and phenological phases derived from satellite (Sentinel-2) data were compared to digital camera-derived data in Paper II. The GCC values obtained from the Sentinel-2 were generally higher than those derived from the camera images. The different viewing angles, the atmospheric effect (the scattering and absorption of radiation due to atmospheric molecules and aerosols) and the consequent correction of the satellite data most probably contributed to the difference. However, the digital camera- and satellite-derived GCC showed similar seasonal patterns. The Sentinel-2 data agreed with the *in situ* observations of a later season start in 2017 at all sites and a lower GCC at Halssiaapa in 2018 compared to other years (Paper II: Fig. 10). The satellite data were scarcer than camera data, and consequently there were larger uncertainties in the function fitted to describe the seasonal course.

The phenology parameters calculated, from the fitted seasonal function showed differences between the satellite and camera-derived data (Paper II: Table 6). The Sentinel-2 data corresponded to an earlier growing season start at Halssiaapa and Kaamanen. At Lompolojänkkä, the satellite-based start-of-season indicator SOS25 and the maximum GCC were estimated to occur later than those obtained from the camera-based data. At Halssiaapa and Kaamanen, the Sentinel-2 data suggested a later occurrence of the end-of-season indicator EOS25, but no systematic difference was found at Lompolojänkkä.

3.2. Studies on the belowground CO_2 fluxes (Papers III and IV)

The peat soil decomposition and PE were determined with isotopic methods (^{14}C and ^{13}C) in laboratory-based studies from two peat soils collected from nutrient-rich and nutrient-poor sites in Papers III and IV.

3.2.1. CO_2 fluxes

According to the bare peat respiration measurements in Paper III, the surface peat generally respired more than the deep peat. The microcosms with planted pine seedlings respired more than the bare peat microcosms. The share of the heterotrophic respiration out of the total soil respiration was calculated as the proportion of bare peat CO_2 production to the total soil CO_2. On average, the bare peat respiration was between 42% and 80% of the total soil respiration (Paper III: Fig. 3). No significant difference between the NR and NP samples was found. The NR surface peat was better soil for the seedling growth (Paper III: Table 1), and thus the average net photosynthesis rates were highest in those seedlings growing in the surface peat microcosms (Paper III: Fig. 2). As stated above, the seedlings growing in surface peat, especially in NR peat, gained also most biomass and the net photosynthesis rate correlated significantly with the mass of the seedlings. The peat and root respiration exceeded the seedling photosynthesis and thus the microcosms were sources of CO_2.

The results of Paper IV show that the basal, control samples of NR peat without nutrient or ^{13}C-glucose addition respired almost twice as much as the basal NP peat and the difference was significant ($p < 0.001$) (Fig. 8). Within the NP peat treatments, the nutrient addition affected the respiration significantly ($p < 0.05$), but not within the NR peat treatments.

3.2.2. Priming effect in peat soil

According to the results of the ^{14}C dating in Paper III, the CO_2 of peat respiration of the microcosms with seedlings was derived from a younger source than the CO_2 respired from the bare peat microcosms (Paper III: Table 2). The results also showed that the CO_2 respired from the NR peat was produced by a younger source than the CO_2 of the NP peat respiration. The NR peat with roots showed on average a bit higher (16%) and the NP peat with roots on average a lower (20%) respiration rates than the bare peat, but these differences were not statistically significant (Figs. 7 and 8). The proportion of the peat respiration to the total soil respiration with roots was 55% in NR peat and 76% in NP peat. The peat respiration was significantly higher (46%) in the NR peat than in the NP peat.

A negative PE was observed in Paper IV for both the NR and NP peat soils; soil respiration of the non-labelled control peat samples was significantly ($p < 0.001$) higher than the calculated soil-derived respiration of the ^{13}C-labelled samples (Fig 8). In the NR peat, the soil-derived respiration rate of the ^{13}C-glucose labelled samples without and with nutrient addition was on average 29.1% and 28.2%, respectively, lower than in the control, non-labelled peat. The corresponding percentages in the NP peat were 39.1% and 33.6%, respectively. The nutrient addition had a significant ($p < 0.001$) impact on the respiration rates in the NP control treatments and on the PE, respiration being higher with nutrient addition. This was not observed for the NR peat.

The calculated ^{13}C-glucose-derived respiration in the beginning of the experiment was significantly higher in the NR peat than in the NP peat, both with and without nutrients (Paper IV: Figs. 1 and 2). No significant difference was found within the different NR or NP peat treatments. It has to be noted that the ^{13}C-glucose-derived respiration declined fast; already on the second measurement day the respiration of NR peat was reduced to 18% and 11%, and the respiration of NP peat to 12% and 7%, without and with nutrient addition, respectively. The calculated cumulative CO_2 flux over 14 days was significantly ($p < 0.001$) higher in the NR peat than in the NP peat.

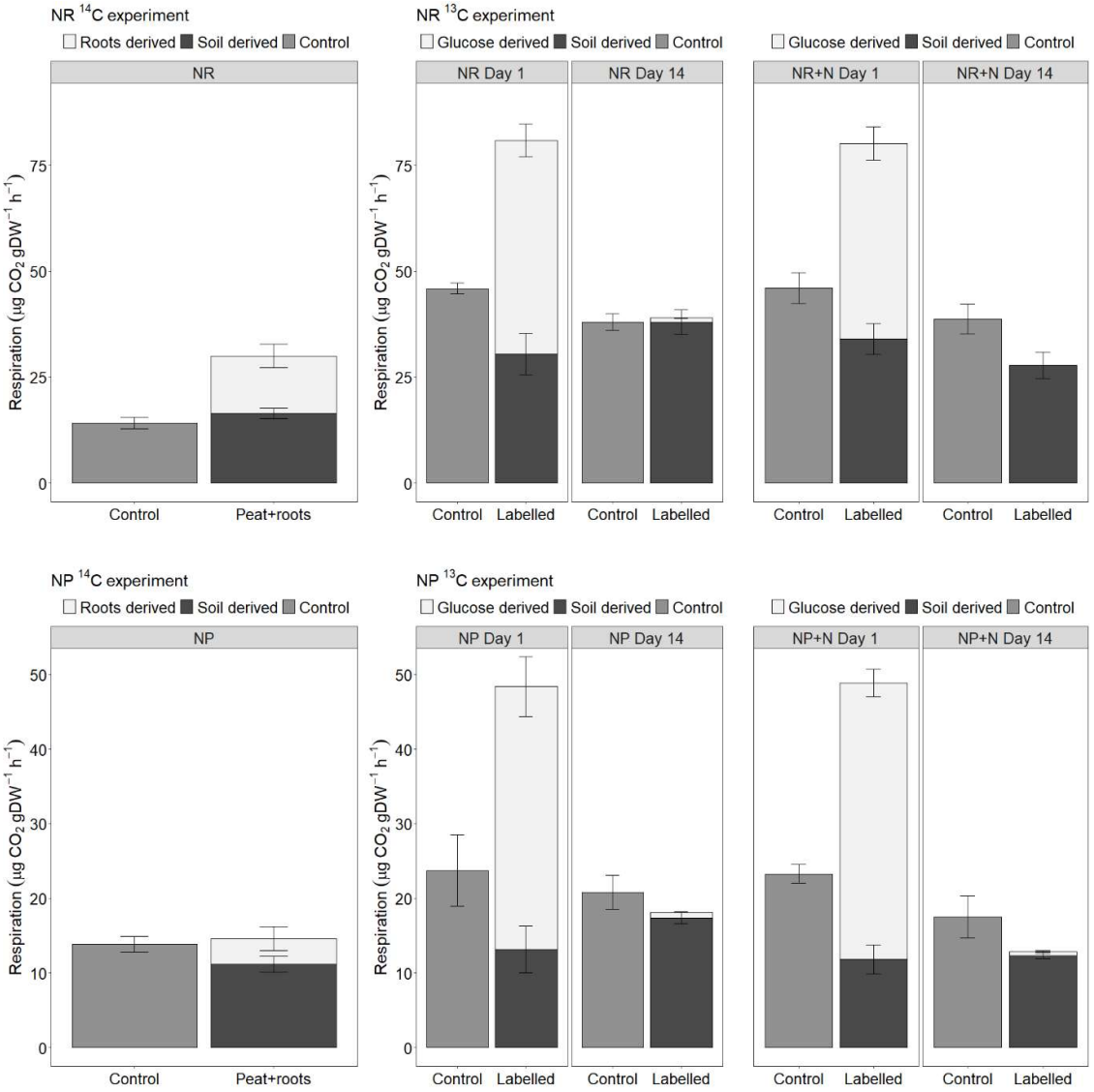

Figure 8. Control peat respiration and the partitioned peat respiration components of NR (above) and NP (below) peat determined in Papers III (left) and IV (right). Respiration was partitioned by the natural abundance method (^{14}C) in Paper III and ^{13}C-glucose labelling in Paper IV. The results from the ^{13}C-labelling and respiration partitioning are shown from the beginning (day 1) and the end (day 14) of the experiment. In the ^{13}C-labelling experiment, additional nutrients (+N) were added to half of the samples. Error bars describe standard deviation (n = 5). Figure modified from Papers III and IV.

3.3. The DOC and DN content, net nitrification rate and microbial biomass C and ^{13}C (Paper IV)

The DOC content did not differ significantly between the NR and NP peat samples or among the different NR peat treatments (Paper IV: Table 2). In contrast, there was a significant difference in the DOC content between different NP treatments ($p < 0.05$): a lower DOC content was observed in the samples with added ^{13}C-glucose. There was no significant difference in the DN content among either the different NR or NP peat treatments, but the DN content was significantly ($p < 0.05$) lower in the ^{13}C-labelled NP peat than in the ^{13}C-labelled NR peat.

The net nitrification rate differed significantly ($p < 0.05$) between the NR and NP samples (Paper IV: Table 2). In the NR peat, net nitrification was detected, while immobilization was observed in the NP peat. In addition, there was a significant difference ($p < 0.05$) between the NP peat samples with and without nutrient addition. Hence, the nutrient addition seemed to further strengthen the observed immobilization.

The ^{13}C-labelled samples had a significantly ($p < 0.05$) higher microbial biomass C (MBC) content than the non-labelled samples (Paper IV: Table 2). The nutrient addition had no significant effect on the MBC content, and the MBC content did not differ between the NR and NP samples. The ^{13}C in MBC (MBC-^{13}C) was lower in the NR peat than in the NR peat, but there was no differences among either the NR or NP treatments. The labelled samples had naturally higher $\delta^{13}C$ values of the MB. The NP peat had in general higher $\delta^{13}C$ values of the MB than the NR peat, but no significant differences were found in mean $\delta^{13}C$ values of the MB between the sites.

4. Discussion

4.1. Studies on the aboveground vegetation greenness (Papers I and II)

Many studies have demonstrated, and this thesis further confirms, that it is possible to detect the development of vegetation greenness of different ecosystems from digital camera-derived images effectively and automatically (e.g., Richardson et al. 2007, 2009, Ahrends et al. 2009, Ide and Oguma 2010, Sonnentag et al. 2012). The derived vegetation indices can be related to changes in the ecosystem–atmosphere CO_2 flux, and they can complement the satellite-based observations (Peichl et al. 2015, Peltoniemi et al. 2018, Vrieling et al. 2018, Koebsch et al. 2020). In the studies of this thesis, clear differences in the green chromatic coordinate (GCC) were found among different sites, years and plant communities and, based on these findings, it can be concluded that vegetation greenness of northern boreal ecosystems can be reliably monitored with digital cameras, even on a plant community level. Currently, studies on the greenness of smaller regions of interest covering, for example, individual plant communities are still scarce. In addition to the small-scale results presented in Paper II, vegetation indices have been derived at the scales of a chamber plot (< 0.5 m^2) (Davidson et al. 2021, Juutinen et al. 2022) and individual trees (Menzel et al. 2015, Cheng et al. 2020).

The highest GCC and photosynthetic productivity (expressed as the GPP_{max}) among the three northern peatlands studied in this thesis were observed at Lompolojänkkä. This site is characterized by high nutrient availability, rich vegetation and a high LAI. In addition, the surface at Lompolojänkkä is the flattest among the study sites, and the stream running through the fen feeds water and nutrients to the fen ecosystem (Lohila et al. 2010, Aurela et al. 2009). At the other peatland sites, i.e., Halssiaapa and Kaamanen, the microtopography is more variable, creating a wide range of hydrological features with differing habitats, which further creates variability in the trophic status and vegetation; especially the string–flark formations impact the species distribution and productivity of plants (Shi et al. 2015). The GCC varied also between different measurement years. The results of Paper II suggest that the annual differences in GCC in the early phase of the growing season were well explained by air temperature, here expressed as a degree day sum. Similar correlation has also been observed for a more southern boreal peatland (Peichl et al. 2015).

Several studies have demonstrated for different ecosystems (forests, grasslands, crops, peatlands) that GPP correlates strongly with a greenness index derived from digital images (Migliavacca et al. 2011, Keenan et al. 2014, Peichl et al. 2015, Toomey et al. 2015, Knox et al. 2017, Järveoja et al. 2018, Peichl et al. 2018, Koebsch et al. 2020). Papers I and II of this thesis confirm this correlation: highly similar seasonal cycles of GCC and the GPP_{max} were observed. Also, related short-term variation in GCC and the GPP_{max} was found, for example, in 2014 and during the drought period in 2018 at Halssiaapa, and in the early part of the growing seasons 2016 and 2017 at Kaamanen. In addition, the results illustrate

that both the maximum GCC and GPP_{max} over the measurement years occurred during the same growing season, but this year differed between the sites Despite these similarities, the regression analysis conducted in Paper II suggests that most of the GPP_{max} variation is associated with the common seasonal cycle rather than GCC as such. This is understandable as green leaf area controls both GCC and GPP and is mainly driven by air temperature and day length (Bauerle et al. 2012, Peichl et al. 2015, Koebsch et al. 2020).

Changes in environmental conditions, such as the timing of the growing season start, mean growing season temperature and warm or cold spells, affect differently not only ecosystems differing in characteristics and habitats but also different plant communities and even different species. For example, Wipf and Rixen (2010) observed that a later start and shorter duration of the growing season decreased the overall plant productivity of arctic and alpine ecosystems. They also noted that the timing of snowmelt had a different effect on different plant functional types; for example, the growth of forbs increased and the growth of grasses decreased with delayed snowmelt. Wipf (2010) stated that the GDDS, rather than the timing of the growing season start, controls the later phenological phases, which also suggests that the conditions prevailing later during the growing season play an important role in the annual plant productivity. The earlier phenological phases, especially for those earlier species that can start their development soon after the snow cover disappears, are more affected by the timing of the snowmelt. The results of this thesis indicate that the vegetation of northern boreal peatlands can quickly start developing after a late growing season start and is capable of reaching the same, or even higher, maximum GCC level, compared to a year with an average spring, if the conditions later in the summer are favourable for vegetation growth. The results in Paper II demonstrate that air temperature (GDDS) is the most important factor in explaining the annual variation of the growing season start dates, which was also observed by Peichl et al. (2015) for a more southern boreal peatland.

As observed by Rinne et al. (2020), the widespread drought detected in 2018 affected the net CO_2 sink of many northern peatland ecosystems. The drought did not affect Lompolojänkkä, however, as WTD did not decrease there, most probably due to the hydrological features of the site. The net CO_2 uptake during the growing season of 2018 even increased at Lompolojänkkä. In contrast, the drought decreased the CO_2 sink of the Kaamanen fen in 2018 (Heiskanen et al. 2021) and, according to the results of Paper II, affected the CO_2 sink even more at Halssiaapa. The GCC at Halssiaapa, derived both from the digital images and the Sentinel-2 satellite data, was lowest in 2018 among the measurement years. Both at Kaamanen and Halssiaapa, WTD was substantially reduced during the drought.

As stated above, the peatland vegetation is often spatially highly variable, and such heterogeneous ecosystems are challenging environments for remote sensing. In Papers I and II of this thesis, it was demonstrated that digital cameras are able to detect differences even at the scale of individual tree crowns and plant communities. In Paper II, the GCC was also derived from the Sentinel-2 satellite data,

and the growing season development was clearly visible in these data, even though the GCC values were generally higher than the camera-based GCC. A similar mismatch between digital camera- and satellite-derived greenness indices has also been observed in other studies (e.g., Liu et al. 2021), and there are various reasons why the GCC derived from these sources can be expected to differ. Vrieling et al. (2018) proposed that the differences result from the non-photosynthetic vegetation mass (dead plant matter, stems, flowers) in the images, which affects the visibility of green biomass in an oblique view. In addition, the camera-derived indices are extracted from raw digital numbers corresponding to the red, green and blue colour channels of the pixels in an image, while satellite-based analysis applies the observed surface reflectance (Vrieling et al. 2018). It has been suggested that images taken at nadir could provide a better correlation with satellite data (Vrieling et al. 2018).

In Paper II, the basic phenological cycle was characterized and different phenological phases were determined by fitting a hyperbolic tangent function to GCC data from both camera and satellite images. The same function was also fitted to GPP data. Large differences were detected in the determined growing season phases between the camera- and satellite-based data, the latter indicating longer growing seasons at Halssiaapa and Kaamanen. Poor satellite data availability deteriorated the fitting and determination of phenological phases, resulting in uncertain parameter estimates, especially in the beginning and end of the growing season. High uncertainty was also involved in the fits of the GPP_{max} at Halssiaapa in 2018 and at Kaamanen in 2019 in the beginning of growing seasons, due to the poor data coverage. While the camera-based monitoring and EC measurements usually produce high-frequency data, the temporal coverage of satellite data is limited; for the study sites of this thesis, a non-cloudy image was produced typically every 5 to 10 days. The satellite data used in Paper II were especially limited in 2016 and 2017, when the Sentinel-2 constellation consisted of a single satellite (Sentinel-2A). Since 2018, the Sentinel-2 satellite data have been available from two satellites (Sentinel-2A and Sentinel-2B).

In addition to observing differences between years and sites, the digital cameras employed in this thesis demonstrated the potential for detecting small-scale and short-term changes in vegetation due to, for example, droughts, as well as for the long-term ecosystem surveillance especially for tracking possible climate change effects. By limiting the images to the scale of a chamber measurement plot, GCC can be related to small-scale measurements of fluxes (Davidson et al. 2021, Juutinen et al. 2022). With the help of GCC observations of differently developing vegetation types, it may be possible to partition a spatially integrated CO_2 flux observation gained from EC measurements into its components separating, for example, the different plant communities within a heterogeneous peatland. The digital image data could also provide support for parameterization of phenological events in ecosystem models and for model evaluation, especially for developing dedicated phenology models incorporated into ecosystem models. Furthermore, the digital camera observations complement the remote sensing data with limited temporal and spatial resolution. For example, continuous digital image data have been used for

verification and interpretation of satellite data (Filippa et al. 2018, Richardson et al. 2007, 2009, Sonnentag et al. 2012).

4.2. Studies on the belowground CO_2 experiments (Papers III and IV)

The basal respiration rates were measured from NR and NP peat samples in Papers III and IV. Although no differences in respiration rates between NR and NP bare peat control samples were detected in Paper III, the peat respiration rate calculated from the total peat and root respiration (i.e., the basal respiration in the presence of vegetation) was 47% higher in the NR peat than in the NP peat. In contrast, the results of Paper IV indicate that the NR control peat without ^{13}C-glucose addition respired significantly more than the NP peat. It must be noted that the peat used for the natural abundance study (Paper III) was incubated for six months before the experiment and thus all the easily decomposable material was supposedly employed, but the peat used in the ^{13}C-labelling study (Paper IV) was fresh. This difference in incubation time, and thus the difference in the amount of easily decomposable C in peat, most likely affected the results of bare peat respiration.

The natural abundance study (Paper III) applying ^{14}C-dating indicated no significant PE in either of the soils. Thus, it was not possible to conclude that the nutrient status of these peat soils affected the PE. However, a negative PE was found in the ^{13}C-glucose addition study (Paper IV) for both peat soils, i.e., for NR and NP peats. In addition, the PE was significantly stronger in the NP peat, implying that the negative PE may be more pronounced in peat soils with less available nutrients. In Paper III, deep, old peat was used for partitioning the respiration to peat- and root-derived components, since the application of the mixing model required a sufficiently large difference in the pMC -values between the two sources. In contrast, only surface peat was used in the ^{13}C-labelling experiment in Paper IV.

The studies on the PE in peat soil are still relatively few and contradictory. The studies have reported both positive (Hamer and Marschner 2002, Basiliko et al. 2012, Hartley et al. 2012, Bader at al. 2018, Walker et al. 2016, Mastný et al. 2021) and negative priming (Bader et al. 2018, Hardie et al. 2011, Yan et al. 2021, Mastný et al. 2021), and some no priming at all (Bader et al. 2018, Leiber-Sauheitl et al. 2015, Aaltonen et al. 2022, Müller et al. 2022). For example, no priming was detected in organic soil by Aaltonen et al. (2022) after glucose addition, by Müller et al. (2022) after artificial root exudate addition and by Leiber-Sauheitl et al. (2015) after the addition of isotopically labelled sheep excrement. In a study conducted on managed organic peat soils, the PE was found to be insignificant in cropland soil, negative in forest soil and positive in grassland soil (Bader et al. 2018). These contrasting results indicate that the PE in peat soils depends on other, probably multiple, variables than land use. Compared to mineral soils, where positive priming has been widely detected (e.g., Luo and Weng 2011, Zimmerman et al. 2011), the organic soils do not seem to support priming the same way as the mineral soils.

As mentioned above, negative PE is believed to result from preferential substrate utilization (Kuzyakov et al. 2000, Kuzyakov 2002, Kuzyakov and Bol 2006, Werth and Kuzyakov 2010, Wang et al. 2015). With nutrient depletion, microbes tend to switch the primary energy source to compounds that are easily available (Kuzyakov 2002, Werth and Kuzyakov 2010, Wang et al. 2015). The results of Paper IV indicate that this was the case in the studied peat soils. In addition, the negative priming was further dampened with higher nutrient availability. The C/N ratio and N content affect the soil fertility and decomposability (e.g., Moore 2002), and Ekblad and Nordgren (2002) suggested that with C/N ratios greater than 30 the activity of microbes is limited. The NP site had a higher C/N ratio (over 30 *in situ*), and while the microbes might therefore be inhibited at the site, the direction of PE did not differ between the sites (Paper IV). However, the negative PE was significantly larger in NP than NR peat, compared to the total amount of CO_2 respired, and the lower nutrient availability seemed to enhance the negative priming.

The results of Paper IV indicate that the microbial biomass was significantly higher in the ^{13}C-labelled samples, although no difference was detected between NR and NP peat. The amount of glucose remaining in the microbes (MBC-^{13}C) after the two-week experiment was significantly higher in NP peat with nutrients and glucose addition than in either of the NR treatments. The proportion of the glucose-derived respiration in the labelled samples was high on the first day, but it decreased rapidly. This suggests that microbes used the fresh and easily decomposable C fast. The amount of respired glucose was lowest in NP peat without added nutrients. These results indicate that the additional C from sugars is used for microbial growth and maintenance instead of respiration, and further confirm the depletion of nutrients in NP peat.

It must be noted that the ^{13}C-glucose used in Paper IV is a simple compound compared to the more complex real root exudates. Wild et al. (2016) reported variable PE results in arctic soils after the addition of different kinds of substrates, and Hamer and Marschner (2002) and Basiliko et al. (2012) reported a positive PE after root exudate addition to peat soil. Nevertheless, the ^{13}C-glucose addition can indicate the short-term potential in the soil microbial reservoir. In addition, the natural bulk peat is a combination of different layers with different degrees of decomposition. Since deep peat was used for the respiration partitioning in Paper III, the results do not entirely represent field conditions. Although most of the roots locate in the active surface layer where litter is gained (Laiho and Finér 1996), the roots and root exudates can also enter deeper peat layers and feed fresh C to these more recalcitrant sections. The results of this thesis could also be applied to re-planted mined peatlands where the plants grow on old, exposed peat. The deep peat is not favourable for the growth of seedlings. This was further verified with the seedling biomass results of Paper III, which showed that the seedling growth rate in surface peat was comparable to that observed for mineral soil by Pumpanen et al. (2009).

Figure 9 summarizes the different C flux components and the role of PE determined for the NR and NP sites. As stated before, the *in situ* CO_2 balances of the study sites indicate that the peat soil at the NR site is a C source, whereas the NP peat soil is a C sink (Lohila et al. 2011, Minkkinen et al. 2018, Kasimir et al. 2021, Korkiakoski et al. 2023). The soil C balance, derived from NEE and tree biomass sequestration indicates that the peat soil at the NR site is annually a net source of C (210 g C m^{-2} yr^{-1}), while the NP soil is a net C sink (-60 g C m^{-2} yr^{-1}) (Fig. 9). The results of Papers III and IV accord with these studies emphasizing the difference between the sites: the decomposition rates are lower in NP peat and simultaneously the negative PE was found to be stronger than in NR peat. The difference in the respiration rates results from differences in the vegetation and litter characteristics and in peat quality and decomposability, indicating that NR peat is more easily decomposable. The observed negative priming might even further inhibit the surface peat decomposition in the NP peat soil in the presence of vegetation. We can conclude that more studies are needed to fully understand the peat decomposition in the presence of roots; especially, the quality of the peat, such as nutrient status, state of humification and C/N ratio, should be taken into account.

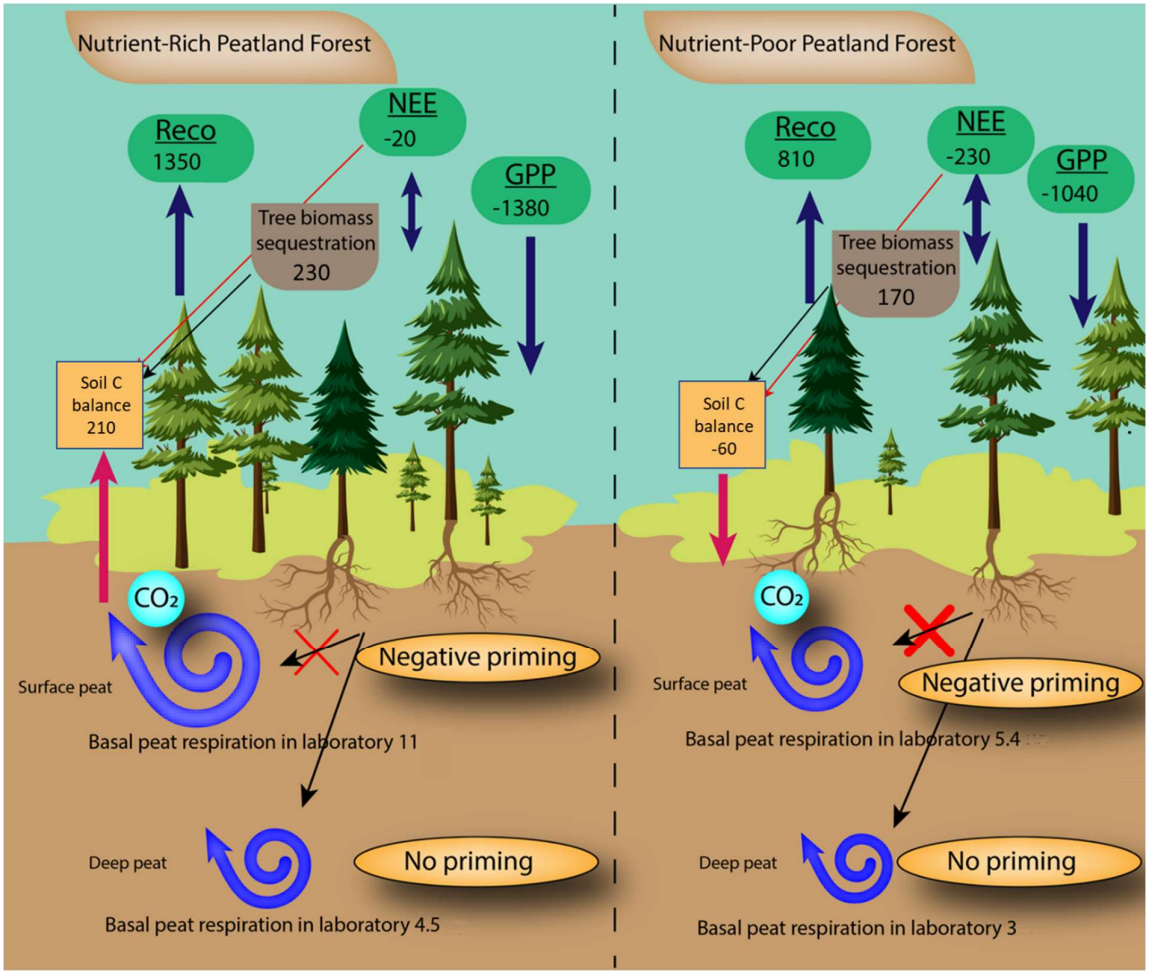

Figure 9. Ecosystem C balance of a nutrient-rich (NR) and a nutrient-poor (NP) forestry-drained peatland in Southern Finland. Net ecosystem exchange (NEE) (sum of gross primary production (GPP) and ecosystem respiration (R_{eco})), and tree biomass sequestration are given in a unit of g C m^{-2} yr^{-1}. The numbers for the NR site are obtained from Korkiakoski et al. (2023) and for the NP site from Minkkinen et al. (2018). The soil C balance was derived from the difference between the annual NEE and tree biomass sequestration. The basal peat respiration (in µg C g DW^{-1} h^{-1}; blue spiral) for surface and deeper peat layers was obtained from laboratory-based isotope (^{13}C and ^{14}C) studies. A negative priming effect (i.e., the decrease in old C decomposition when fresh C is added to the soil; red cross) was found in surface peat, while no significant priming (i.e., no change in old C decomposition) was found in deeper peat. The size of the arrows, crosses and spirals approximates the strength of the flux or effect. Figure modified from Paper IV.

4.3. Applications of the results

Earth system, ecosystem and ecosystem process models provide a means to predict how ecosystems respond to climate and land-use changes, in addition to describing the functioning and interactions of ecosystem components. Modelling results are also utilized in policy making, and thus the reliability of these predictions is important. Both vegetation phenology and the PE are affected by climate and land-use change, and both have feedbacks on climate. Hence, integrating them to ecosystem models could improve policy-relevant predictions (Richardson et al. 2012, Cheng et al. 2014, Perveen et al. 2014).

However, the underlying mechanisms driving both phenology and the PE are still not completely understood, which hinders model development (Piao et al. 2019, Bernard et al. 2022).

While satellite-derived phenology-related data have been used in process and ecosystem-level modelling (e.g., Viskari et al. 2015, Dokoohaki et al. 2022, Nevalainen et al. 2022), the camera-derived data have been utilized less frequently. Digital camera-derived greenness indices have been employed for modelling phenology and for simulating daily GPP (Migliavacca et al. 2011, Zhou et al. 2013, Knox et al. 2017). Knox et al. (2017) compared greenness indices in a light-use efficiency model and found that satellite-derived data resulted in a poorer data–model agreement than camera-derived data at a wetland site with heterogeneous surface (open water and vegetation), while for a more homogeneous wetland the model performed well with both data. It has been shown that species-level observations are highly useful for developing vegetation phenology models from the community to ecosystem scale (Tang et al. 2016, Piao et al. 2019). Piao et al. (2019) also acknowledge that there are differences in phenological phases between plant-level and remote sensing observations, as also observed in this thesis between camera- and satellite-derived data. This further emphasizes the need for high-resolution and high-frequency digital camera data.

As Dietze et al. (2018) suggest, ecological forecasting is critically needed to understand how ecosystems will respond to changing climate, for example to predict the changes in phenological and biogeochemical cycles. Automated, high-resolution and real-time data production is needed for developing robust tools for ecological forecasting (Besson et al. 2022). For example, Nevalainen et al. (2022) designed a near-term forecast system to monitor agricultural C sequestration, in which the forecast is adjusted with CO_2 fluxes and satellite-derived LAI observations. Since digital cameras can produce greenness data more frequently than satellites, these kinds of forecasts could potentially be improved with the continuous data obtained from repeat photography. This thesis has amply demonstrated the availability and validity of such data.

Data for model development are not only needed on the aboveground phenology, but also the belowground phenology is just as important (Piao et al. 2019). A study addressing the root phenology implies that the effects of climate change may affect the above- and belowground phenology differently (Blume-Werry et al. 2016), and the belowground phenology is moreover connected to root exudate-driven processes, such as the PE. Conceptual models with a timescale from hours to days describing the soil C decomposition have been integrated to global land biosphere models, but the interaction between labile and recalcitrant C has been mostly dismissed (Guenet et al. 2016). In some studies, however, the PE has been integrated to process and ecosystem models (Cheng et al. 2014, Perveen et al. 2014, Guenet et al. 2016, Bastida et al. 2019, Liu et al. 2020). Cheng et al. (2014) and Perveen et al. (2014) demonstrated that it is possible to incorporate the PE into ecosystem models with additional parameters and thus improve the accuracy of predictions. In addition, Guenet et al. (2016) introduced a

simple conceptual model for priming, which reproduces priming experiments conducted in the laboratory and in the field. Recently, Liu et al. (2020) presented a mechanistic model which predicts the soil C replenishment and PE and the processes contributing to them, such as litter input and decomposition. Since the PE and its drivers are still not fully understood, the rhizosphere process is difficult to model. However, as Bernard et al. (2022) suggest, the objectives of PE modelling should be divided into two groups: firstly, understanding the PE and secondly, quantifying the PE.

It is worth noting that all of the sites studied in this thesis located in the boreal zone and are mostly peatland habitats, which obviously restricts the representativeness of the results presented. For example, it has been previously reported that the GCC of evergreen forests show a weaker correlation with GPP during the early growing season than ecosystems with deciduous vegetation (Toomey et al. 2015, Wingate et al. 2015). This accords with the results of Paper I, which show that forest site there was more fluctuation in the correlation between GCC and CO_2 flux data at the evergreen than at the peatland site, although the GCC and photosynthesis developed simultaneously also at the forest site. The PE studies of this thesis were conducted with soil sampled from forestry-drained peatlands and as discussed above, previous PE studies have reported contradictory results with differently managed organic soils, thus it is difficult to estimate the representativeness of the results of this thesis. It has to be also noted that the laboratory-based peat decomposition studies do not completely represent natural conditions. Further studies combining different methodologies would be needed to gain more knowledge about the PE in peat soils.

5. Conclusions

In this thesis, both above- and belowground CO_2 fluxes were examined with process-specific methods to support standardized flux measurements by additional information. In Papers I and II, digital repeat photography was evaluated as a method for monitoring vegetation greenness and development. The digital camera setup was capable of detecting even small-scale differences and changes in vegetation, in addition to producing continuous data for long-term ecosystem monitoring. Differences in vegetation dynamics were detected between two adjacent ecosystems, three pristine peatlands and different plant communities within a peatland site. The differences in GCC were found to be associated with the nutrient availability and vegetation composition at the site or within the region of interest. The seasonal vegetation greenness data derived from digital cameras were combined with seasonal CO_2 flux measurements. Although the seasonal development of GCC and CO_2 uptake were correlated, the short-term variation in GCC did not in general explain the corresponding variation in the daily maximum GPP.

Differences in vegetation dynamics were also observed between different measurement years. The peatland vegetation was demonstrated to compensate for the late growing season start; the maximum daily maximum GPP over the measurement years was reached during a summer with the latest growing season start. The effect of drought on GCC and the daily maximum GPP was observed to depend on the hydrological features of the site. The camera- and satellite-derived GCC data indicated the same seasonal cycle, but the poorer temporal resolution of the satellite data undermined the reliable determination of the timing of different phenological phases.

In Papers III and IV, the soil CO_2 fluxes and PE of two forestry-drained peatlands were examined in the laboratory with isotope techniques. The basal surface peat respiration and the peat respiration in the presence of plants were significantly higher in the more nutrient-rich peat soil. The results are in accordance with the observed differences in the CO_2 balances at the sites from which the peat samples were collected: the peat soil has been observed to lose C at the nutrient-rich site and accumulate C at the nutrient-poor site. This emphasizes the difference in the quality of the peat between the sites, which is a result of vegetation and litter quality. In these studies, no priming (^{14}C-experiment) or negative priming (^{13}C-experiment) was found. Thus, it can be concluded that the addition of fresh C (in the form of seedling roots or glucose) did not increase, or it even decreased, the old peat decomposition. The negative priming was more pronounced in the peat soil with less available nutrients.

This thesis demonstrated that the phenology cameras are a useful method for tracking changes in ecosystem greenness, including both the seasonal course and shorter-term perturbances due to extreme weather conditions. In the long term, repeat photography provides a tool for monitoring the possible effects of climate change. In addition to monitoring, the phenology camera-derived data could be used in ecosystem models and in model evaluation, as well as for verification of satellite data. Importantly,

the changes in the aboveground ecosystem affect the belowground processes. Although climate warming and peatland drainage are likely to increase the rate of peat decomposition, the results of this thesis indicate that the fresh C addition from increasing biomass and root exudates, for example, does not further enhance old peat decompositionin the studied forestry-drained peatlands. Since the PE contributes to C cycling, further studies on the PE mechanisms and related ecosystem and process modelling would be important, although this presents a major challenge. However, this thesis showed that these process-specific methods for studying above- and belowground CO_2 fluxes improve our understanding of ecosystem C balances, which is necessary for assessing the effects of climate change and human-induced land-use changes.

References

Aaltonen, H., Zhu, X., Khatun, R., Laurén, A., Palviainen, M., Könönen, M., Peltomaa, E., Berninger, F., Köster, K., Ojala, A., & Pumpanen, J. (2022). The effects of glucose addition and water table manipulation on peat quality of drained peatland forests with different management practices. *Soil Science Society of America Journal*, *86*(6), 1625–1638. https://doi.org/10.1002/saj2.20419

Ahrends, H. E., Etzold, S., Kutsch, W. L., Stoeckli, R., Bruegger, R., Jeanneret, F., Wanner, H., Buchmann, N., & Eugster, W. (2009). Tree phenology and carbon dioxide fluxes: Use of digital photography for process-based interpretation at the ecosystem scale. *Climate Research*, *39*, 261–274. https://doi.org/10.3354/cr00811

Aitkenhead, J. A. & McDowell, W. H. (2000). Soil C:N ratio as a predictor of annual riverine DOC flux at local and global scales. *Global Biogeochemical Cycles*, *14*(1), 127–138. https://doi.org/10.1029/1999GB900083

Aurela, M., Tuovinen, J.-P., & Laurila, T. (1998). Carbon dioxide exchange in a subarctic peatland ecosystem in northern Europe measured by the eddy covariance technique. *Journal of Geophysical Research: Atmospheres*, *103*(D10), 11289–11301. https://doi.org/10.1029/98JD00481

Aurela, M., Lohila, A., Tuovinen, J.-P., Hatakka, J., Riutta, T., & Laurila, T. (2009). Carbon dioxide exchange on a northern boreal fen. *Boreal Environment Research*, *14*, 699–710.

Bader, C., Müller, M., Szidat, S., Schulin, R., & Leifeld, J. (2018). Response of peat decomposition to corn straw addition in managed organic soils. *Geoderma*, *v. 309*, 75–83. https://doi.org/10.1016/j.geoderma.2017.09.001

Baggs, E. M. (2006). Partitioning the components of soil respiration: A research challenge. *Plant and Soil*, *284*(1), 1–5. https://doi.org/10.1007/s11104-006-0047-7

Baldocchi, D. D. (2003). Assessing the eddy covariance technique for evaluating carbon dioxide exchange rates of ecosystems: Past, present and future. *Global Change Biology*, *9*(4), 479–492. https://doi.org/10.1046/j.1365-2486.2003.00629.x

Basiliko, N., Stewart, H., Roulet, N. T., & Moore, T. R. (2012). Do root exudates enhance peat decomposition? *Geomicrobiology Journal*, *29*(4), 374–378. https://doi.org/10.1080/01490451.2011.568272

Bastida, F., García, C., Fierer, N., Eldridge, D. J., Bowker, M. A., Abades, S., Alfaro, F. D., Asefaw Berhe, A., Cutler, N. A., Gallardo, A., García-Velázquez, L., Hart, S. C., Hayes, P. E., Hernández, T., Hseu, Z.-Y., Jehmlich, N., Kirchmair, M., Lambers, H., Neuhauser, S., Peña-Ramírez, V. M., Pérez, C. A., Reed, A. C., Santos, F., Siebe, C., Sullivan, B. W., Trivedi, P., Vera, A., Williams, M. A., Moreno, J. L., & Delgado-Baquerizo, M. (2019). Global ecological predictors of the soil priming effect. *Nature Communications*, *10*(1), 3481. https://doi.org/10.1038/s41467-019-11472-7

Bauerle, W. L., Oren, R., Way, D. A., Qian, S. S., Stoy, P. C., Thornton, P. E., Bowden, J. D., Hoffman, F. M., & Reynolds, R. F. (2012). Photoperiodic regulation of the seasonal pattern of photosynthetic capacity and the implications for carbon cycling. *Proceedings of the National Academy of Sciences*, *109*(22), 8612. https://doi.org/10.1073/pnas.1119131109

Belyea, L. R., & Malmer, N. (2004). Carbon sequestration in peatland: Patterns and mechanisms of response to climate change. *Global Change Biology*, *10*(7), 1043–1052. https://doi.org/10.1111/j.1529-8817.2003.00783.x

Bernard, L., Basile-Doelsch, I., Derrien, D., Fanin, N., Fontaine, S., Guenet, B., Karimi, B., Marsden, C., & Maron, P.-A. (2022). Advancing the mechanistic understanding of the priming effect on soil organic matter mineralisation. *Functional Ecology*, *36*(6), 1355–1377. https://doi.org/10.1111/1365-2435.14038

Berninger, F. (1997). Effects of drought and phenology on GPP in Pinus sylvestris: A simulation study along a geographical gradient. *Functional Ecology*, *11*(1), 33–42.

Besson, M., Alison, J., Bjerge, K., Gorochowski, T. E., Høye, T. T., Jucker, T., Mann, H. M. R., & Clements, C. F. (2022). Towards the fully automated monitoring of ecological communities. *Ecology Letters*, *25*(12), 2753–2775. https://doi.org/10.1111/ele.14123

Biasi, C., Tavi, N. M., Jokinen, S., Shurpali, N., Hämäläinen, K., Jungner, H., Oinonen, M., & Martikainen, P. J. (2011). Differentiating sources of CO_2 from organic soil under bioenergy crop cultivation: A field-based approach using 14C. *Soil Biology and Biochemistry*, *43*(12), 2406–2409. https://doi.org/10.1016/j.soilbio.2011.08.003

Black, T. A., Chen, W. J., Barr, A. G., Arain, M. A., Chen, Z., Nesic, Z., Hogg, E. H., Neumann, H. H., & Yang, P. C. (2000). Increased carbon sequestration by a boreal deciduous forest in years with a warm spring. *Geophysical Research Letters*, *27*(9), 1271–1274. https://doi.org/10.1029/1999GL011234

Blagodatskaya, E., & Kuzyakov, Y. (2008). Mechanisms of real and apparent priming effects and their dependence on soil microbial biomass and community structure: Critical review. *Biology and Fertility of Soils*, *45*(2), 115–131. https://doi.org/10.1007/s00374-008-0334-y

Blume-Werry, G., Wilson, S. D., Kreyling, J., & Milbau, A. (2016). The hidden season: Growing season is 50% longer below than above ground along an arctic elevation gradient. *New Phytologist*, *209*(3), 978–986. https://doi.org/10.1111/nph.13655

Bryant, R. G., & Baird, A. J. (2003). The spectral behaviour of Sphagnum canopies under varying hydrological conditions. *Geophysical Research Letters*, *30*(3). https://doi.org/10.1029/2002GL016053

Bubier, J. L., Frolking, S., Crill, P. M., & Linder, E. (1999). Net ecosystem productivity and its uncertainty in a diverse boreal peatland. *Journal of Geophysical Research: Atmospheres*, *104*(D22), 27683–27692. https://doi.org/10.1029/1999JD900219

Canadell, J.G., Monteiro, P.M.S., Costa, M. H., Cotrim da Cunha, L., Cox, P. M., Eliseev, A. V., Henson, S., Ishii, M., Jaccard, S., Koven, C., Lohila, A., Patra, P. K., Piao, S., Rogelj, J., Syampungani, S., Zaehle, S., & Zickfeld, K. (2021). Global carbon and other biogeochemical cycles and feedbacks supplementary material. In *Climate change 2021: The physical science basis. Contribution of working group I to the sixth assessment report of the Intergovernmental Panel on Climate Change*. Masson-Delmotte, V., Zhai, P., Pirani, A., Connors, S. L., Péan, C., Berger, S., Caud, N., Chen, Y., Goldfarb, L., Gomis, M. I., Huang, M., Leitzell, K., Lonnoy, E., Matthews, J. B. R., Maycock, T. K., Waterfield, T., Yelekçi, O., Yu, R., & Zhou B. (eds.). Available from https://www.ipcc.ch/

Chapin, F. S., Woodwell, G. M., Randerson, J. T., Rastetter, E. B., Lovett, G. M., Baldocchi, D. D., Clark, D. A., Harmon, M. E., Schimel, D. S., Valentini, R., Wirth, C., Aber, J. D., Cole, J. J., Goulden, M. L., Harden, J. W., Heimann, M., Howarth, R. W., Matson, P. A., McGuire, A. D., Melillo, J. M., Mooney, H. A., Neff, J. C., Houghton, R. A., Pace, M. L., Ryan, M. G., Running, S. W., Sala, O. E., Schlesinger, W. H. & Schulze, E.-D. (2006). Reconciling carbon-cycle concepts, terminology, and methods. *Ecosystems*, *9*(7), 1041–1050. https://doi.org/10.1007/s10021-005-0105-7

Cheng, W., Parton, W. J., Gonzalez-Meler, M. A., Phillips, R., Asao, S., McNickle, G. G., Brzostek, E., & Jastrow, J. D. (2014). Synthesis and modeling perspectives of rhizosphere priming. *New Phytologist*, *201*(1), 31–44. https://doi.org/10.1111/nph.12440

Cheng, Y., Vrieling, A., Fava, F., Meroni, M., Marshall, M., & Gachoki, S. (2020). Phenology of short vegetation cycles in a Kenyan rangeland from PlanetScope and Sentinel-2. *Remote Sensing of Environment*, *248*, 112004. https://doi.org/10.1016/j.rse.2020.112004

Clymo, R. S., Turunen, J., & Tolonen, K. (1998). Carbon accumulation in peatland. *Oikos*, *81*(2), 368–388. JSTOR. https://doi.org/10.2307/3547057

Crowther, T. W., Todd-Brown, K. E. O., Rowe, C. W., Wieder, W. R., Carey, J. C., Machmuller, M. B., Snoek, B. L., Fang, S., Zhou, G., Allison, S. D., Blair, J. M., Bridgham, S. D., Burton, A. J., Carrillo, Y., Reich, P. B., Clark, J. S., Classen, A. T., Dijkstra, F. A., Elberling, B., Emmet, B. A., Estiarte, M., Frey, S. D., Guo, J., Harte, J., Jiang, L., Johnson, B. R., Kröel-Dulay, G., Larsen, K. S., Laudon, H., Lavellee, J. M., Luo, Y., Lupascu, M., Ma, L. N., Marhan, S., Michelsen, A., Mohan, J., Niu, S., Pendall, E., Peñuelas, J., Pfeifer-Meister, L., Poll, C., Reinsch, S., Reynolds, L. L., Schmidt, I. K., Sistla, S., Sokol, N. W., Templer, P. H., Treseder, K. K., Welker, J. M., & Bradford, M. A. (2016). Quantifying global soil carbon losses in response to warming. *Nature*, *540*(7631), 104–108. https://doi.org/10.1038/nature20150

Davidson, S. J., Goud, E. M., Malhotra, A., Estey, C. O., Korsah, P., & Strack, M. (2021). Linear disturbances shift boreal peatland plant communities toward earlier peak Greenness. *Journal of Geophysical Research: Biogeosciences*, *126*(8), e2021JG006403. https://doi.org/10.1029/2021JG006403

Delbart, N., Picard, G., Le Toan, T., Kergoat, L., Quegan, S., Woodward, I., Dye, D., & Fedotova, V. (2008). Spring phenology in boreal Eurasia over a nearly century time scale. *Global Change Biology*, *14*(3), 603–614. https://doi.org/10.1111/j.1365-2486.2007.01505.x

Dietze, M. C., Fox, A., Beck-Johnson, L. M., Betancourt, J. L., Hooten, M. B., Jarnevich, C. S., Keitt, T. H., Kenney, M. A., Laney, C. M., Larsen, L. G., Loescher, H. W., Lunch, C. K., Pijanowski, B. C., Randerson, J. T., Read, E. K., Tredennick, A. T., Vargas, R., Weathers, K. C., & White, E. P. (2018). Iterative near-term ecological forecasting: Needs, opportunities, and challenges. *Proceedings of the National Academy of Sciences*, *115*(7), 1424–1432. https://doi.org/10.1073/pnas.1710231115

Dijkstra, F., Carrillo, Y., Pendall, E., & Morgan, J. (2013). Rhizosphere priming: A nutrient perspective. *Frontiers in Microbiology*, *4*, 216. https://doi.org/10.3389/fmicb.2013.00216

Dokoohaki, H., Morrison, B. D., Raiho, A., Serbin, S. P., Zarada, K., Dramko, L., & Dietze, M. (2022). Development of an open-source regional data assimilation system in PEcAn v. 1.7.2: Application to carbon cycle reanalysis across the contiguous US using SIPNET. *Geosci. Model Dev.*, *15*(8), 3233–3252. https://doi.org/10.5194/gmd-15-3233-2022

Ekblad, A., & Nordgren, A. (2002). Is growth of soil microorganisms in boreal forests limited by carbon or nitrogen availability? *Plant and Soil*, *242*(1), 115–122. https://doi.org/10.1023/A:1019698108838

Fatichi, S., Leuzinger, S., & Körner, C. (2014). Moving beyond photosynthesis: From carbon source to sink-driven vegetation modeling. *New Phytologist*, *201*(4), 1086–1095. https://doi.org/10.1111/nph.12614

Filippa, G., Cremonese, E., Migliavacca, M., Galvagno, M., Sonnentag, O., Humphreys, E., Hufkens, K., Ryu, Y., Verfaillie, J., Morra di Cella, U., & Richardson, A. D. (2018). NDVI derived from near-infrared-enabled digital cameras: Applicability across different plant functional types. *Agricultural and Forest Meteorology*, *249*, 275–285. https://doi.org/10.1016/j.agrformet.2017.11.003

Frolking, S. E., Bubier, J. L., Moore, T. R., Ball, T., Bellisario, L. M., Bhardwaj, A., Carroll, P., Crill, P. M., Lafleur, P. M., McCaughey, J. H., Roulet, N. T., Suyker, A. E., Verma, S. B., Waddington, J. M., & Whiting, G. J. (1998). Relationship between ecosystem productivity and photosynthetically active radiation for northern peatlands. *Global Biogeochemical Cycles*, *12*(1), 115–126. https://doi.org/10.1029/97GB03367

Fry, B. (2006). *Stable Isotope Ecology*. Springer, New York, NY.

Gajewski, K., Viau, A., Sawada, M., Atkinson, D., & Wilson, S. (2001). Sphagnum peatland distribution in North America and Eurasia during the past 21,000 years. *Global Biogeochemical Cycles*, *15*(2), 297–310. https://doi.org/10.1029/2000GB001286

Gallego-Sala, A. V., Charman, D. J., Brewer, S., Page, S. E., Prentice, I. C., Friedlingstein, P., Moreton, S., Amesbury, M. J., Beilman, D. W., Björck, S., Blyakharchuk, T., Bochicchio, C., Booth, R. K., Bunbury, J., Camill, P., Carless, D., Chimner, R. A., Clifford, M., Cressey, E., Courtney-Mustaphi, C., De Vleeschouwer, F., de Jong, R., Fialkiewicz-Koziel, B., Finkelstein, S. A., Garneau, M., Githumbi, E., Hribjlan, J., Holquist, J., Hughes, P. D. M., Jones, C., Jones, M. C., Karofeld, E., Klein, E. S., Kokfelt, U., Korhola, A., Lacourse, T., Le Roux, G., Lamentowicz, M., Large, D., Lavoie, M., Loisel, J., Mackay, H., MacDonald, G. M., Makila, M., Magnan, G., Marchant, R., Marcisz, K., Martinez Cortizas, A., Massa, C., Mathijssen, P., Mauquoy, D., Mighall, T., Mitchell, F. J. G., Moss, P., Nichols, J., Oksanen, P. O., Orme, L., Packalen, M. S., Robinson, S., Roland, T. P., Sanderson, N. K., Sannel, A. B. K., Silva-Sánchez, N., Steinberg, N., Swindles, G. T., Turner, T. E., Uglow, J., Väliranta, M., van Bellen, S., van der Linden, M., van Geel, B., Wang, G., Yu, Z., Zaragoza-Castells, J., & Zhao, Y. (2018). Latitudinal limits to the predicted increase of the peatland carbon sink with warming. *Nature Climate Change*, *8*(10), 907–913. https://doi.org/10.1038/s41558-018-0271-1

Gavazov, K., Albrecht, R., Buttler, A., Dorrepaal, E., Garnett, M. H., Gogo, S., Hagedorn, F., Mills, R. T. E., Robroek, B. J. M., & Bragazza, L. (2018). Vascular plant-mediated controls on atmospheric carbon assimilation and peat carbon decomposition under climate change. *Global Change Biology*, *24*(9), 3911–3921. https://doi.org/10.1111/gcb.14140

Gorham, E. (1991). Northern Peatlands: Role in the Carbon Cycle and Probable Responses to Climatic Warming. *Ecological Applications*, *1*(2), 182–195. https://doi.org/10.2307/1941811

Guenet, B., Leloup, J., Raynaud, X., Bardoux, G., & Abbadie, L. (2010). Negative priming effect on mineralization in a soil free of vegetation for 80 years. *European Journal of Soil Science*, *61*(3), 384–391. https://doi.org/10.1111/j.1365-2389.2010.01234.x

Guenet, B., Moyano, F. E., Peylin, P., Ciais, P., & Janssens, I. A. (2016). Towards a representation of priming on soil carbon decomposition in the global land biosphere model ORCHIDEE (version 1.9.5.2). *Geoscientific Model Development*, *9*(2), 841–855. https://doi.org/10.5194/gmd-9-841-2016

Hahn, V., Högberg, P., & Buchmann, N. (2006). ^{14}C – a tool for separation of autotrophic and heterotrophic soil respiration. *Global Change Biology*, *12*(6), 972–982. https://doi.org/10.1111/j.1365-2486.2006.001143.x

Hamer, U., & Marschner, B. (2002). Priming effects of sugars, amino acids, organic acids and catechol on the mineralization of lignin and peat. *Journal of Plant Nutrition and Soil Science*, *165*(3), 261–268. https://doi.org/10.1002/1522-2624(200206)165:3<261::AID-JPLN261>3.0.CO;2-I

Hanson, P. J., Edwards, N. T., Garten, C. T., & Andrews, J. A. (2000). Separating root and soil microbial contributions to soil respiration: A review of methods and observations. *Biogeochemistry*, *48*(1), 115–146. https://doi.org/10.1023/A:1006244819642

Hardie, S. M. L., Garnett, M. H., Fallick, A. E., Rowland, A. P., & Flowers, T. H. (2011). Abiotic drivers and their interactive effect on the flux and carbon isotope (^{14}C and $\delta^{13}C$) composition of peat-respired CO_2. *Soil Biology and Biochemistry*, *43*, 2432–2440. https://doi.org/10.1016/j.soilbio.2011.08.010

Harenda, K. M., Lamentowicz, M., Samson, M., & Chojnicki, B. H. (2018). The Role of Peatlands and Their Carbon Storage Function in the Context of Climate Change. In T. Zielinski, I. Sagan, & W. Surosz (Eds.), *Interdisciplinary Approaches for Sustainable Development Goals:*

Economic Growth, Social Inclusion and Environmental Protection (pp. 169–187). Springer International Publishing. https://doi.org/10.1007/978-3-319-71788-3_12

Hartley, I. P., Garnett, M. H., Sommerkorn, M., Hopkins, D. W., Fletcher, B. J., Sloan, V. L., Phoenix, G. K., & Wookey, P. A. (2012). A potential loss of carbon associated with greater plant growth in the European Arctic. *Nature Climate Change*, *2*(12), 875–879. https://doi.org/10.1038/nclimate1575

Heimann, M., & Reichstein, M. (2008). Terrestrial ecosystem carbon dynamics and climate feedbacks. *Nature*, *451*(7176), 289–292. https://doi.org/10.1038/nature06591

Heinonsalo, J., Jørgensen, K. S., & Sen, R. (2001). Microcosm-based analyses of Scots pine seedling growth, ectomycorrhizal fungal community structure and bacterial carbon utilization profiles in boreal forest humus and underlying illuvial mineral horizons. *FEMS Microbilogy Ecology*, *36*(1), 73–84. https://doi.org/10.1111/j.1574-6941.2001.tb00827.x

Heiskanen, L., Tuovinen, J.-P., Räsänen, A., Virtanen, T., Juutinen, S., Lohila, A., Penttilä, T., Linkosalmi, M., Mikola, J., Laurila, T., & Aurela, M. (2021). Carbon dioxide and methane exchange of a patterned subarctic fen during two contrasting growing seasons. *Biogeosciences*, *18*(3), 873–896. https://doi.org/10.5194/bg-18-873-2021

Hopkins, F., Gonzalez-Meler, M. A., Flower, C. E., Lynch, D. J., Czimczik, C., Tang, J., & Subke, J.-A. (2013). Ecosystem-level controls on root-rhizosphere respiration. *New Phytologist*, *199*(2), 339–351. https://doi.org/10.1111/nph.12271

Hämäläinen, K., Fritze, H., Jungner, H., Karhu, K., Oinonen, M., Sonninen, E., Spetz, P., Tuomi, M., Vanhala, P., & Liski, J. (2010). Molecular sieve sampling of CO_2 from decomposition of soil organic matter for AMS radiocarbon measurements. *Nuclear Instruments Methods B*, *268*, 1067–1069. https://doi.org/10.1016/j.nimb.2009.10.099

Högberg, P., Nordgren, A., Buchmann, N., Taylor, A. F. S., Ekblad, A., Högberg, M. N., Nyberg, G., Ottosson-Löfvenius, M., & Read, D. J. (2001). Large-scale forest girdling shows that current photosynthesis drives soil respiration. *Nature*, *411*(6839), 789–792. https://doi.org/10.1038/35081058

Högberg, P., & Read, D. J. (2006). Towards a more plant physiological perspective on soil ecology. *Trends in Ecology & Evolution*, *21*(10), 548–554. https://doi.org/10.1016/j.tree.2006.06.004

Ide, R., & Oguma, H. (2010). Use of digital cameras for phenological observations. *Special Issue on Advances of Ecological Remote Sensing Under Global Change*, *5*(5), 339–347. https://doi.org/10.1016/j.ecoinf.2010.07.002

Jaatinen, K., Fritze, H., Laine, J., & Laiho, R. (2007). Effects of short- and long-term water-level drawdown on the populations and activity of aerobic decomposers in a boreal peatland. *Global Change Biology*, *13*(2), 491–510. https://doi.org/10.1111/j.1365-2486.2006.01312.x

Järveoja, J., Nilsson, M. B., Gažovič, M., Crill, P. M., & Peichl, M. (2018). Partitioning of the net CO_2 exchange using an automated chamber system reveals plant phenology as key control of production and respiration fluxes in a boreal peatland. *Global Change Biology*, *24*(8), 3436–3451. https://doi.org/10.1111/gcb.14292

Jones, M. C., Harden, J., O'Donnell, J., Manies, K., Jorgenson, T., Treat, C., & Ewing, S. (2017). Rapid carbon loss and slow recovery following permafrost thaw in boreal peatlands. *Global Change Biology*, *23*(3), 1109–1127. https://doi.org/10.1111/gcb.13403

Juutinen, S., Aurela, M., Tuovinen, J.-P., Ivakhov, V., Linkosalmi, M., Räsänen, A., Virtanen, T., Mikola, J., Nyman, J., Vähä, E., Loskutova, M., Makshtas, A., & Laurila, T. (2022). Variation in CO_2 and CH_4 fluxes among land cover types in heterogeneous Arctic tundra in northeastern Siberia. *Biogeosciences*, *19*(13), 3151–3167. https://doi.org/10.5194/bg-19-3151-2022

Kasimir, Å., He, H., Jansson, P.-E., Lohila, A., & Minkkinen, K. (2021). Mosses are important for soil carbon sequestration in forested peatlands. *Frontiers in Environmental Science*, *9*. https://doi.org/10.3389/fenvs.2021.680430

Keeling, C. D., Chin, J. F. S., & Whorf, T. P. (1996). Increased activity of northern vegetation inferred from atmospheric CO_2 measurements. *Nature*, *382*(6587), 146–149. https://doi.org/10.1038/382146a0

Keenan, T. F., Gray, J., Friedl, M. A., Toomey, M., Bohrer, G., Hollinger, D. Y., Munger, J. W., O'Keefe, J., Schmid, H. P., Wing, I. S., Yang, B., & Richardson, A. D. (2014). Net carbon uptake has increased through warming-induced changes in temperate forest phenology. *Nature Climate Change*, *4*(7), 598–604. https://doi.org/10.1038/nclimate2253

Keys, A. J., Perry, M. A. J., & Lawlor, D. W. (1994). What controls photosynthesis? *Biochemical Society Transactions*, *22*(4), 1016–1020. https://doi.org/10.1042/bst0221016

Knox, S. H., Dronova, I., Sturtevant, C., Oikawa, P. Y., Matthes, J. H., Verfaillie, J., & Baldocchi, D. (2017). Using digital camera and Landsat imagery with eddy covariance data to model gross primary production in restored wetlands. *Agricultural and Forest Meteorology*, *237–238*, 233–245. https://doi.org/10.1016/j.agrformet.2017.02.020

Koebsch, F., Sonnentag, O., Järveoja, J., Peltoniemi, M., Alekseychik, P., Aurela, M., Arslan, A. N., Dinsmore, K., Gianelle, D., Helfter, C., Jackowicz-Korczynski, M., Korrensalo, A., Leith, F., Linkosalmi, M., Lohila, A., Lund, M., Maddison, M., Mammarella, I., Mander, Ü., Minkkinen, K., Pickard, A., Pullens, J. W. M., Tuittila, E.-S., Nilsson, M. B., & Peichl, M. (2020). Refining the role of phenology in regulating gross ecosystem productivity across European peatlands. *Global Change Biology*, *26*(2), 876–887. https://doi.org/10.1111/gcb.14905

Korkiakoski, M., Ojanen, P., Tuovinen, J.-P., Minkkinen, K., Nevalainen, O., Penttilä, T., Aurela, M., Laurila, T., & Lohila, A. (2023). Partial cutting of a boreal nutrient-rich peatland forest causes radically less short-term on-site CO_2 emissions than clear-cutting. *Agricultural and Forest Meteorology*, *332*, 109361. https://doi.org/10.1016/j.agrformet.2023.109361

Körner, C. & Basler, D. (2010). Phenology under global warming. *Science*, *327*(5972), 1461–1462. https://doi.org/10.1126/science.1186473

Krüger, J. P., Alewell, C., Minkkinen, K., Szidat, S., & Leifeld, J. (2016). Calculating carbon changes in peat soils drained for forestry with four different profile-based methods. *Forest Ecology and Management*, *381*, 29–36. https://doi.org/10.1016/j.foreco.2016.09.006

Kuhry, P. & Turunen, J. (2006). The Postglacial Development of Boreal and Subarctic Peatlands. In R. K. Wieder & D. H. Vitt (Eds.), *Boreal Peatland Ecosystems* (pp. 25–46). Springer Berlin Heidelberg. https://doi.org/10.1007/978-3-540-31913-9_3

Kuzyakov, Y. (2002). Separating microbial respiration of exudates from root respiration in non-sterile soils: A comparison of four methods. *Soil Biology and Biochemistry*, *34*(11), 1621–1631. https://doi.org/10.1016/S0038-0717(02)00146-3

Kuzyakov, Y. (2006). Sources of CO_2 efflux from soil and review of partitioning methods. *Soil Biology and Biochemistry*, *38*(3), 425–448. https://doi.org/10.1016/j.soilbio.2005.08.020

Kuzyakov, Y. (2010). Priming effects: Interactions between living and dead organic matter. *Soil Biology and Biochemistry*, *42*(9), 1363–1371. https://doi.org/10.1016/j.soilbio.2010.04.003

Kuzyakov, Y., & Bol, R. (2006). Sources and mechanisms of priming effect induced in two grassland soils amended with slurry and sugar. *Soil Biology and Biochemistry*, *38*(4), 747–758. https://doi.org/10.1016/j.soilbio.2005.06.025

Kuzyakov, Y., & Cheng, W. (2001). Photosynthesis controls of rhizosphere respiration and organic matter decomposition. *Soil Biology and Biochemistry*, *33*(14), 1915–1925. https://doi.org/10.1016/S0038-0717(01)00117-1

Kuzyakov, Y., Friedel, J. K., & Stahr, K. (2000). Review of mechanisms and quantification of priming effects. *Soil Biology and Biochemistry*, *32*(11), 1485–1498. https://doi.org/10.1016/S0038-0717(00)00084-5

Kuzyakov, Y., Hill, P. W., & Jones, D. L. (2007). Root exudate components change litter decomposition in a simulated rhizosphere depending on temperature. *Plant and Soil*, *290*(1), 293–305. https://doi.org/10.1007/s11104-006-9162-8

Laiho, R. (2006). Decomposition in peatlands: Reconciling seemingly contrasting results on the impacts of lowered water levels. *Soil Biology and Biochemistry*, *38*(8), 2011–2024. https://doi.org/10.1016/j.soilbio.2006.02.017

Laiho, R., & Finér, L. (1996). Changes in root biomass after water-level drawdown on pine mires in southern Finland. *Scandinavian Journal of Forest Research*, *11*(1–4), 251–260. https://doi.org/10.1080/02827589609382934

Laiho, R., Vasander, H., Penttilä, T., & Laine, J. (2003). Dynamics of plant-mediated organic matter and nutrient cycling following water-level drawdown in boreal peatlands. *Global Biogeochemical Cycles*, *17*(2). https://doi.org/10.1029/2002GB002015

Leiber-Sauheitl, K., Fuß, R., Burkart, S., Buegger, F., Dänicke, S., Meyer, U., Petzke, K. J., & Freibauer, A. (2015). Sheep excreta cause no positive priming of peat-derived CO_2 and N_2O emissions. *Soil Biology & Biochemistry*, *88*, 282–293. https://doi.org/10.1016/j.soilbio.2015.06.001

Limpens, J., Berendse, F., Blodau, C., Canadell, J. G., Freeman, C., Holden, J., Roulet, N., Rydin, H., & Schaepman-Strub, G. (2008). Peatlands and the carbon cycle: From local processes to global implications – a synthesis. *Biogeosciences*, *5*(5), 1475–1491. https://doi.org/10.5194/bg-5-1475-2008

Linkosalo, T., Häkkinen, R., Terhivuo, J., Tuomenvirta, H., & Hari, P. (2009). The time series of flowering and leaf bud burst of boreal trees (1846–2005) support the direct temperature observations of climatic warming. *Agricultural and Forest Meteorology*, *149*(3), 453–461. https://doi.org/10.1016/j.agrformet.2008.09.006

Liu, K., Xu, Y., Feng, W., Zhang, X., Yao, S., & Zhang, B. (2020). Modeling the dynamics of protected and primed organic carbon in soil and aggregates under constant soil moisture following litter incorporation. *Soil Biology and Biochemistry*, *151*, 108039. https://doi.org/10.1016/j.soilbio.2020.108039

Liu, N., Garcia, M., Singh, A., Clare, J. D. J., Stenglein, J. L., Zuckerberg, B., Kruger, E. L., & Townsend, P. A. (2021). Trail camera networks provide insights into satellite-derived phenology for ecological studies. *International Journal of Applied Earth Observation and Geoinformation*, *97*, 102291. https://doi.org/10.1016/j.jag.2020.102291

Lohila, A., Aurela, M., Hatakka, J., Pihlatie, M., Minkkinen, K., Penttilä, T., & Laurila, T. (2010). Responses of N_2O fluxes to temperature, water table and N deposition in a northern boreal fen. *European Journal of Soil Science*, *61*(5), 651–661. https://doi.org/10.1111/j.1365-2389.2010.01265.x

Lohila, A., Minkkinen, K., Aurela, M., Tuovinen, J.-P., Penttilä, T., Ojanen, P., & Laurila, T. (2011). Greenhouse gas flux measurements in a forestry-drained peatland indicate a large carbon sink. *Biogeosciences*, *8*(11), 3203–3218. https://doi.org/10.5194/bg-8-3203-2011

Loisel, J., Gallego-Sala, A. V., Amesbury, M. J., Magnan, G., Anshari, G., Beilman, D. W., Benavides, J. C., Blewett, J., Camill, P., Charman, D. J., Chawchai, S., Hedgpeth, A., Kleinen, T., Korhola, A., Large, D., Mansilla, C. A., Müller, J., van Bellen, S., West, J. B., Yu, Z., Bubier, J. L., Garneau, M., Moore, T., Sannel, A. B. K., Page, S., Väliranta, M., Bechtold, M., Brovkin, V., Cole, L. E. S., Chanton, J. P., Christensen, T. R., Davies, M. A., De Vleeschouwer, F., Finkelstein, S. A., Frolking, S., Gałka, M., Gandois, L., Girkin, N., Harris, L. I., Heinemeyer, A., Hoyt, A. M., Jones, M. C., Joos, F., Juutinen, S., Kaiser, K., Lacourse, T., Lamentowicz, M., Larmola, T., Leifeld, J., Lohila, A., Milner, A. M., Minkkinen, K., Moss, P., Naafs, B. D. A., Nichols, J., O'Donnell, J., Payne, R., Philben, M., Piilo, S., Quillet, A., Ratnayake, A. S., Roland, T. P., Sjögersten, S., Sonnentag, O., Swindles, G. T., Swinnen, W., Talbot, J., Treat, C., Valach, A. C., & Wu, J. (2021). Expert assessment of future vulnerability of the global peatland carbon sink. *Nature Climate Change*, *11*(1), 70–77. https://doi.org/10.1038/s41558-020-00944-0

Luo, Y., & Weng, E. (2011). Dynamic disequilibrium of the terrestrial carbon cycle under global change. *Trends in Ecology & Evolution*, *26*(2), 96–104. https://doi.org/10.1016/j.tree.2010.11.003

Maanavilja, L., Riutta, T., Aurela, M., Pulkkinen, M., Laurila, T., & Tuittila, E.-S. (2011). Spatial variation in CO_2 exchange at a northern aapa mire. *Biogeochemistry*, *104*(1), 325–345. https://doi.org/10.1007/s10533-010-9505-7

Maljanen, M., Sigurdsson, B. D., Guðmundsson, J., Óskarsson, H., Huttunen, J. T., & Martikainen, P. J. (2010). Greenhouse gas balances of managed peatlands in the Nordic countries – present knowledge and gaps. *Biogeosciences*, *7*(9), 2711–2738. https://doi.org/10.5194/bg-7-2711-2010

Martikainen, P. J., Nykänen, H., Alm, J., & Silvola, J. (1995). Change in fluxes of carbon dioxide, methane and nitrous oxide due to forest drainage of mire sites of different trophy. *Plant and Soil*, *168*(1), 571–577. https://doi.org/10.1007/BF00029370

Mastný, J., Bárta, J., Kaštovská, E., & Picek, T. (2021). Decomposition of peatland DOC affected by root exudates is driven by specific r and K strategic bacterial taxa. *Scientific Reports*, *11*(1), 18677. https://doi.org/10.1038/s41598-021-97698-2

Menzel, A., Helm, R., & Zang, C. (2015). Patterns of late spring frost leaf damage and recovery in a European beech (Fagus sylvatica L.) stand in south-eastern Germany based on repeated digital photographs. *Frontiers in Plant Science*, *6*. https://doi.org/10.3389/fpls.2015.00110

Meroni, M., Verstraete, M. M., Rembold, F., Urbano, F., & Kayitakire, F. (2014). A phenology-based method to derive biomass production anomalies for food security monitoring in the Horn of Africa. *International Journal of Remote Sensing*, *35*(7), 2472–2492. https://doi.org/10.1080/01431161.2014.883090

Migliavacca, M., Galvagno, M., Cremonese, E., Rossini, M., Meroni, M., Sonnentag, O., Cogliati, S., Manca, G., Diotri, F., Busetto, L., Cescatti, A., Colombo, R., Fava, F., Morra di Cella, U., Pari, E., Siniscalco, C., & Richardson, A. D. (2011). Using digital repeat photography and eddy covariance data to model grassland phenology and photosynthetic CO_2 uptake. *Agricultural and Forest Meteorology*, *151*(10), 1325–1337. https://doi.org/10.1016/j.agrformet.2011.05.012

Migliavacca, M., Sonnentag, O., Keenan, T. F., Cescatti, A., O'Keefe, J., & Richardson, A. D. (2012). On the uncertainty of phenological responses to climate change, and implications for a terrestrial biosphere model. *Biogeosciences*, *9*(6), 2063–2083. https://doi.org/10.5194/bg-9-2063-2012

Minkkinen, K., & Laine, J. (1998). Long-term effect of forest drainage on the peat carbon stores of pine mires in Finland. *Canadian Journal of Forest Research*, *28*(9), 1267–1275. https://doi.org/10.1139/x98-104

Minkkinen, K., Ojanen, P., Penttilä, T., Aurela, M., Laurila, T., Tuovinen, J.-P., & Lohila, A. (2018). Persistent carbon sink at a boreal drained bog forest. *Biogeosciences*, *15*(11), 3603–3624. https://doi.org/10.5194/bg-15-3603-2018

Minkkinen, K., Vasander, H., Jauhiainen, S., Karsisto, M., & Laine, J. (1999). Post-drainage changes in vegetation composition and carbon balance in Lakkasuo mire, Central Finland. *Plant and Soil*, *207*(1), 107–120. https://doi.org/10.1023/A:1004466330076

Moore, P. D. (2002). The future of cool temperate bogs. *Environmental Conservation*, *29*(1), 3–20. Cambridge Core. https://doi.org/10.1017/S0376892902000024

Moore, T., & Basiliko, N. (2006). Decomposition in boreal peatlands. In R. K. Wieder & D. H. Vitt (Eds.), *Boreal Peatland Ecosystems* (pp. 125–143). Springer Berlin Heidelberg. https://doi.org/10.1007/978-3-540-31913-9_7

Müller, R., Maier, A., Inselsbacher, E., Peticzka, R., Wang, G., & Glatzel, S. (2022). ^{13}C-labeled artificial root exudates are immediately respired in a peat mesocosm study. *Diversity*, *14*(9). https://doi.org/10.3390/d14090735

Nevalainen, O., Niemitalo, O., Fer, I., Juntunen, A., Mattila, T., Koskela, O., Kukkamäki, J., Höckerstedt, L., Mäkelä, L., Jarva, P., Heimsch, L., Vekuri, H., Kulmala, L., Stam, Å., Kuusela, O., Gerin, S., Viskari, T., Vira, J., Hyväluoma, J., Tuovinen, J.-P., Lohila, A., Laurila, T., Heinonsalo, J., Aalto, T., Kunttu, I., & Liski, J. (2022). Towards agricultural soil carbon monitoring, reporting, and verification through the Field Observatory Network (FiON). *Geoscientific Instrumentation, Methods and Data Systems*, *11*(1), 93–109. https://doi.org/10.5194/gi-11-93-2022

Nordli, Ø., Wielgolaski, F. E., Bakken, A. K., Hjeltnes, S. H., Måge, F., Sivle, A., & Skre, O. (2008). Regional trends for bud burst and flowering of woody plants in Norway as related to climate change. *International Journal of Biometeorology*, *52*(7), 625–639. https://doi.org/10.1007/s00484-008-0156-5

Ojanen, P., Lehtonen, A., Heikkinen, J., Penttilä, T., & Minkkinen, K. (2014). Soil CO_2 balance and its uncertainty in forestry-drained peatlands in Finland. *Forest Ecology and Management*, *325*, 60–73. https://doi.org/10.1016/j.foreco.2014.03.049

Ojanen, P., Minkkinen, K., & Penttilä, T. (2013). The current greenhouse gas impact of forestry-drained boreal peatlands. *Forest Ecology and Management*, *289*, 201–208. https://doi.org/10.1016/j.foreco.2012.10.008

Palonen, V., & Oinonen, M. (2013). Molecular sieves in $^{14}CO_2$ sampling and handling. *Radiocarbon*, *55*, 416–420. https://doi.org/10.2458/ azu_js_rc.55.16335

Park, T., Ganguly, S., Tømmervik, H., Euskirchen, E. S., Høgda, K.-A., Karlsen, S. R., Brovkin, V., Nemani, R. R., & Myneni, R. B. (2016). Changes in growing season duration and productivity of northern vegetation inferred from long-term remote sensing data. *Environmental Research Letters*, *11*(8), 084001. https://doi.org/10.1088/1748-9326/11/8/084001

Paterson, E., Midwood, A. J., & Millard, P. (2009). Through the eye of the needle: A review of isotope approaches to quantify microbial processes mediating soil carbon balance. *New Phytologist*, *184*(1), 19–33. https://doi.org/10.1111/j.1469-8137.2009.03001.x. PMID: 19740278.

Peichl, M., Gažovič, M., Vermeij, I., de Goede, E., Sonnentag, O., Limpens, J., & Nilsson, M. B. (2018). Peatland vegetation composition and phenology drive the seasonal trajectory of maximum gross primary production. *Scientific Reports*, *8*(1), 8012. https://doi.org/10.1038/s41598-018-26147-4

Peichl, M., Sonnentag, O., & Nilsson, M. B. (2015). Bringing Color into the Picture: Using Digital Repeat Photography to Investigate Phenology Controls of the Carbon Dioxide Exchange in a Boreal Mire. *Ecosystems*, *18*(1), 115–131. https://doi.org/10.1007/s10021-014-9815-z

Peltoniemi, K., Fritze, H., & Laiho, R. (2009). Response of fungal and actinobacterial communities to water-level drawdown in boreal peatland sites. *Soil Biology and Biochemistry*, *41*(9). https://doi.org/10.1016/j.soilbio.2009.06.018

Peltoniemi, K., Straková, P., Fritze, H., Iráizoz, P. A., Pennanen, T., & Laiho, R. (2012). How water-level drawdown modifies litter-decomposing fungal and actinobacterial communities in boreal peatlands. *Soil Biology and Biochemistry*, *51*, 20–34. https://doi.org/10.1016/j.soilbio.2012.04.013

Peltoniemi, M., Aurela, M., Böttcher, K., Kolari, P., Loehr, J., Karhu, J., Linkosalmi, M., Tanis, C. M., Tuovinen, J.-P., & Arslan, A. N. (2018). Webcam network and image database for studies of phenological changes of vegetation and snow cover in Finland, image time series from 2014 to 2016. *Earth System Science Data*, *10*(1), 173–184. https://doi.org/10.5194/essd-10-173-2018

Perveen, N., Barot, S., Alvarez, G., Klumpp, K., Martin, R., Rapaport, A., Herfurth, D., Louault, F., & Fontaine, S. (2014). Priming effect and microbial diversity in ecosystem functioning and response to global change: A modeling approach using the SYMPHONY model. *Global Change Biology*, *20*(4), 1174–1190. https://doi.org/10.1111/gcb.12493

Petach, A. R., Toomey, M., Aubrecht, D. M., & Richardson, A. D. (2014). Monitoring vegetation phenology using an infrared-enabled security camera. *Agricultural and Forest Meteorology*, *195–196*, 143–151. https://doi.org/10.1016/j.agrformet.2014.05.008

Piao, S., Liu, Q., Chen, A., Janssens, I. A., Fu, Y., Dai, J., Liu, L., Lian, X., Shen, M., & Zhu, X. (2019). Plant phenology and global climate change: Current progresses and challenges. *Global Change Biology*, *25*(6), 1922–1940. https://doi.org/10.1111/gcb.14619

Pudas, E., Leppälä, M., Tolvanen, A., Poikolainen, J., Venäläinen, A., & Kubin, E. (2008). Trends in phenology of Betula pubescens across the boreal zone in Finland. *International Journal of Biometeorology*, *52*(4), 251–259. https://doi.org/10.1007/s00484-007-0126-3

Pumpanen, J. S., Heinonsalo, J., Rasilo, T., Hurme, K.-R., & Ilvesniemi, H. (2009). Carbon balance and allocation of assimilated CO_2 in Scots pine, Norway spruce, and Silver birch seedlings determined with gas exchange measurements and ^{14}C pulse labelling. *Trees*, *23*(3), 611–621. https://doi.org/10.1007/s00468-008-0306-8

Päivänen, J., & Hånell, B. (2012). *Peatland ecology and forestry – a sound approach* (Vol. 3). Helsingin yliopiston metsätieteiden laitos.

Richardson, A. D., Anderson, R. S., Arain, M. A., Barr, A. G., Bohrer, G., Chen, G., Chen, J. M., Ciais, P., Davis, K. J., Desai, A. R., Dietze, M. C., Dragoni, D., Garrity, S. R., Gough, C. M., Grant, R., Hollinger, D. Y., Margolis, H. A., McCaughey, H., Migliavacca, M., Monson, R. K., Munger, J. W., Poulter, B., Raczka, B. M., Ricciuto, D. M., Sahoo, A. K., Schaefer, K., Tian, H., Vargas, R., Verbeeck, H., Xiao, J., & Xue, Y. (2012). Terrestrial biosphere models need better representation of vegetation phenology: Results from the North American Carbon Program Site Synthesis. *Global Change Biology*, *18*(2), 566–584. https://doi.org/10.1111/j.1365-2486.2011.02562.x

Richardson, A. D., Hollinger, D. Y., Dail, D. B., Lee, J. T., Munger, J. W., & O'Keefe, J. (2009). Influence of spring phenology on seasonal and annual carbon balance in two contrasting New England forests. *Tree Physiology*, *29*(3), 321–331. https://doi.org/10.1093/treephys/tpn040

Richardson, A. D., Jenkins, J. P., Braswell, B. H., Hollinger, D. Y., Ollinger, S. V., & Smith, M.-L. (2007). Use of digital webcam images to track spring green-up in a deciduous broadleaf forest. *Oecologia*, *152*(2), 323–334. https://doi.org/10.1007/s00442-006-0657-z

Richardson, A. D., Keenan, T. F., Migliavacca, M., Ryu, Y., Sonnentag, O., & Toomey, M. (2013). Climate change, phenology, and phenological control of vegetation feedbacks to the climate

system. *Agricultural and Forest Meteorology*, *169*, 156–173. https://doi.org/10.1016/j.agrformet.2012.09.012

Rinne, J., Tuovinen, J.-P., Klemedtsson, L., Aurela, M., Holst, J., Lohila, A., Weslien, P., Vestin, P., Łakomiec, P., Peichl, M., Tuittila, E.-S., Heiskanen, L., Laurila, T., Li, X., Alekseychik, P., Mammarella, I., Ström, L., Crill, P., & Nilsson, M. B. (2020). Effect of the 2018 European drought on methane and carbon dioxide exchange of northern mire ecosystems. *Philosophical Transactions of the Royal Society B: Biological Sciences*, *375*(1810), 20190517. https://doi.org/10.1098/rstb.2019.0517

Rydin, H., & Jeglum, J. K. (2013). *The Biology of Peatlands* (2nd ed.). Oxford University Press. https://doi.org/10.1093/acprof:osobl/9780199602995.001.0001

Scheffer, R. A., & Aerts, R. (2000). Root decomposition and soil nutrient and carbon cycling in two temperate fen ecosystems. *Oikos*, *91*(3), 541–549. https://doi.org/10.1034/j.1600-0706.2000.910316.x

Shi, X., Thornton, P. E., Ricciuto, D. M., Hanson, P. J., Mao, J., Sebestyen, S. D., Griffiths, N. A., & Bisht, G. (2015). Representing northern peatland microtopography and hydrology within the Community Land Model. *Biogeosciences*, *12*(21), 6463–6477. https://doi.org/10.5194/bg-12-6463-2015

Simola, H., Pitkänen, A., & Turunen, J. (2012). Carbon loss in drained forestry peatlands in Finland, estimated by re-sampling peatlands surveyed in the 1980s. *European Journal of Soil Science*, *63*(6), 798–807. https://doi.org/10.1111/j.1365-2389.2012.01499.x

Sonnentag, O., Detto, M., Vargas, R., Ryu, Y., Runkle, B. R. K., Kelly, M., & Baldocchi, D. D. (2011). Tracking the structural and functional development of a perennial pepperweed (Lepidium latifolium L.) infestation using a multi-year archive of webcam imagery and eddy covariance measurements. *Agricultural and Forest Meteorology*, *151*(7), 916–926. https://doi.org/10.1016/j.agrformet.2011.02.011

Sonnentag, O., Hufkens, K., Teshera-Sterne, C., Young, A. M., Friedl, M., Braswell, B. H., Milliman, T., O'Keefe, J., & Richardson, A. D. (2012). Digital repeat photography for phenological research in forest ecosystems. *Agricultural and Forest Meteorology*, *152*, 159–177. https://doi.org/10.1016/j.agrformet.2011.09.009

Stén, C.-G. (1998). *The mires and usefulness of peat in Tammela, southern Finland (in Finnish, abstract in English).* (No. 314; Report of Peat Investigation). Geological Survey of Finland.

Straková, P., Anttila, J., Spetz, P., Kitunen, V., Tapanila, T., & Laiho, R. (2010). Litter quality and its response to water level drawdown in boreal peatlands at plant species and community level. *Plant and Soil*, *335*(1), 501–520. https://doi.org/10.1007/s11104-010-0447-6

Subke, J.-A., Hahn, V., Battipaglia, G., Linder, S., Buchmann, N., & Cotrufo, M. F. (2004). Feedback interactions between needle litter decomposition and rhizosphere activity. *Oecologia*, *139*(4), 551–559. https://doi.org/10.1007/s00442-004-1540-4

Subke, J.-A., Inglima, I., & Francesca Cotrufo, M. (2006). Trends and methodological impacts in soil CO2 efflux partitioning: A metaanalytical review. *Global Change Biology*, *12*(6), 921–943. https://doi.org/10.1111/j.1365-2486.2006.01117.x

Tang, J., Körner, C., Muraoka, H., Piao, S., Shen, M., Thackeray, S. J., & Yang, X. (2016). Emerging opportunities and challenges in phenology: A review. *Ecosphere*, *7*(8), e01436. https://doi.org/10.1002/ecs2.1436

Tanis, C. M., Peltoniemi, M., Linkosalmi, M., Aurela, M., Böttcher, K., Manninen, T., & Arslan, A. N. (2018). A system for acquisition, processing and visualization of image time series from multiple camera networks. *Data*, *3*(23). https://doi.org/10.3390/data3030023

Toomey, M., Friedl, M. A., Frolking, S., Hufkens, K., Klosterman, S., Sonnentag, O., Baldocchi, D. D., Bernacchi, C. J., Biraud, S. C., Bohrer, G., Brzostek, E., Burns, S. P., Coursolle, C., Hollinger, D. Y., Margolis, H. A., McCaughey, H., Monson, R. K., Munger, J. W., Pallardy, S., Phillips, R. P., Torn, M. S., Wharton, S., Zeri, M., & Richardson, A. D. (2015). Greenness indices from digital cameras predict the timing and seasonal dynamics of canopy-scale photosynthesis. *Ecological Applications*, *25*(1), 99–115. https://doi.org/10.1890/14-0005.1

Trumbore, S. (2006). Carbon respired by terrestrial ecosystems – recent progress and challenges. *Global Change Biology*, *12*(2), 141–153. https://doi.org/10.1111/j.1365-2486.2006.01067.x

Turetsky, M., Wieder, K., Halsey, L., & Vitt, D. (2002). Current disturbance and the diminishing peatland carbon sink. *Geophysical Research Letters*, *29*(11), 21–1. https://doi.org/10.1029/2001GL014000

Turunen, J. (2008). *Development of Finnish peatland area and carbon storage 1950–2000*. http://hdl.handle.net/10138/234741

Turunen, J., Tomppo, E., Tolonen, K., & Reinikainen, A. (2002). Estimating carbon accumulation rates of undrained mires in Finland–application to boreal and subarctic regions. *The Holocene*, *12*(1), 69–80. https://doi.org/10.1191/0959683602hl522rp

Vasander, H., & Kettunen, A. (2006). Carbon in Boreal Peatlands. In R. K. Wieder & D. H. Vitt (Eds.), *Boreal Peatland Ecosystems* (pp. 165–194). Springer Berlin Heidelberg. https://doi.org/10.1007/978-3-540-31913-9_9

Viskari, T., Hardiman, B., Desai, A. R., & Dietze, M. C. (2015). Model-data assimilation of multiple phenological observations to constrain and predict leaf area index. *Ecological Applications*, *25*(2), 546–558. https://doi.org/10.1890/14-0497.1

Vitt, D. H., & Wieder, R. K. (2006). Boreal Peatland Ecosystems: Our Carbon Heritage. In R. K. Wieder & D. H. Vitt (Eds.), *Boreal Peatland Ecosystems* (pp. 165–194). Springer Berlin Heidelberg. https://doi.org/10.1007/978-3-540-31913-9_9

Vrieling, A., Meroni, M., Darvishzadeh, R., Skidmore, A. K., Wang, T., Zurita-Milla, R., Oosterbeek, K., O'Connor, B., & Paganini, M. (2018). Vegetation phenology from Sentinel-2 and field cameras for a Dutch barrier island. *Remote Sensing of Environment*, *215*, 517–529. https://doi.org/10.1016/j.rse.2018.03.014

Walker, T. N., Garnett, M. H., Ward, S. E., Oakley, S., Bardgett, R. D., & Ostle, N. J. (2016). Vascular plants promote ancient peatland carbon loss with climate warming. *Global Change Biology*, *22*(5), 1880–1889. PubMed. https://doi.org/10.1111/gcb.13213

Wang, H., Boutton, T. W., Xu, W., Hu, G., Jiang, P., & Bai, E. (2015). Quality of fresh organic matter affects priming of soil organic matter and substrate utilization patterns of microbes. *Scientific Reports*, *5*(1), 10102. https://doi.org/10.1038/srep10102

Werth, M., & Kuzyakov, Y. (2010). ^{13}C fractionation at the root–microorganisms–soil interface: A review and outlook for partitioning studies. *Soil Biology and Biochemistry*, *42*(9), 1372–1384. https://doi.org/10.1016/j.soilbio.2010.04.009

Wild, B., Gentsch, N., Čapek, P., Diáková, K., Alves, R. J. E., Bárta, J., Gittel, A., Hugelius, G., Knoltsch, A., Kuhry, P., Lashchinskiy, N., Mikutta, R., Palmtag, J., Schleper, C., Schnecker, J., Shibistova, O., Takriti, M., Torsvik, V. L., Urich, T., Watzka, M., Šantrůčková, H., Guggenberger, G., & Richter, A. (2016). Plant-derived compounds stimulate the decomposition of organic matter in arctic permafrost soils. *Scientific Reports*, *6*(1), 25607. https://doi.org/10.1038/srep25607

Wingate, L., Ogée, J., Cremonese, E., Filippa, G., Mizunuma, T., Migliavacca, M., Moisy, C., Wilkinson, M., Moureaux, C., Wohlfahrt, G., Hammerle, A., Hörtnagl, L., Gimeno, C., Porcar-

Castell, A., Galvagno, M., Nakaji, T., Morison, J., Kolle, O., Knohl, A., Kutsch, W., Kolari, P., Nikinmaa, E., Ibrom, A., Gielen, B., Eugster, W., Balzarolo, M., Papale, D., Klumpp, K., Köstner, B., Grünwald, T., Joffre, R., Ourcival, J.-M., Hellstrom, M., Lindroth, A., Geroge, C., Longdoz, B., Genty, B., Levula, J., Heinesch, B., Sprintsin, M., Yakir, D., Manise, T., Guyon, D., Ahrends, H., Plaza-Aguilar, A., Guan, J. H., & Grace, J. (2015). Interpreting canopy development and physiology using a European phenology camera network at flux sites. *Biogeosciences*, *12*(20), 5995–6015. https://doi.org/10.5194/bg-12-5995-2015

Wipf, S. (2010). Phenology, growth, and fecundity of eight subarctic tundra species in response to snowmelt manipulations. *Plant Ecology*, *207*(1), 53–66. https://doi.org/10.1007/s11258-009-9653-9

Wipf, S., & Rixen, C. (2010). A review of snow manipulation experiments in Arctic and alpine tundra ecosystems. *Polar Research*, *29*(1), 95–109. https://doi.org/10.3402/polar.v29i1.6054

Xu, J., Morris, P. J., Liu, J., & Holden, J. (2018). PEATMAP: Refining estimates of global peatland distribution based on a meta-analysis. *CATENA*, *160*, 134–140. https://doi.org/10.1016/j.catena.2017.09.010

Yan, W., Wang, Y., Ju, P., Huang, X., & Chen, H. (2022). Water level regulates the rhizosphere priming effect on SOM decomposition of peatland soil. *Rhizosphere*, *21*, 100455. https://doi.org/10.1016/j.rhisph.2021.100455

Zhou, L., He, H., Sun, X., Zhang, L., Yu, G., Ren, X., Wang, J., & Zhao, F. (2013). Modeling winter wheat phenology and carbon dioxide fluxes at the ecosystem scale based on digital photography and eddy covariance data. *Ecological Informatics*, *18*, 69–78. https://doi.org/10.1016/j.ecoinf.2013.05.003

Zimmerman, A. R., Gao, B., & Ahn, M.-Y. (2011). Positive and negative carbon mineralization priming effects among a variety of biochar-amended soils. *Soil Biology and Biochemistry*, *43*(6), 1169–1179. https://doi.org/10.1016/j.soilbio.2011.02.005